AD-A115 760 NAVAL AIR DEVELOPMENT CENTER WARMINSTER PA AIRCRAFT --ETC F/G 11/4
LOW VELOCITY, TRANSVERSE NORMAL IMPACT OF A CLAMPED PLATE.(U)
OCT 81 R E LLORENS, L W GAUSE
UNCLASSIFIED NADC-81250-60 NL

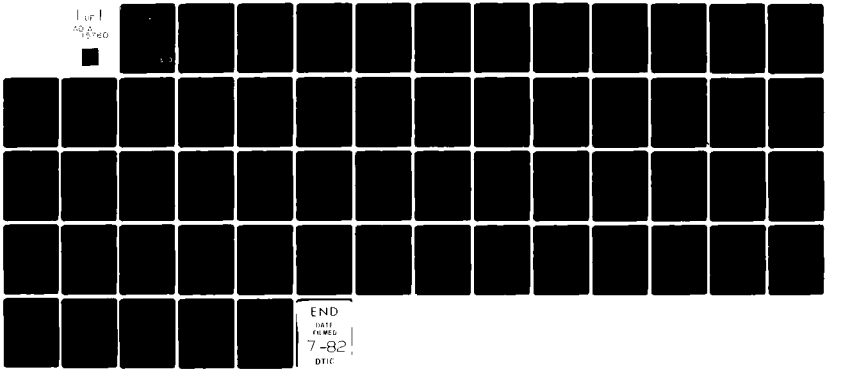

END
DATE FILMED
7-82
DTIC

(12)

REPORT NO. NADC-81250-60

LOW VELOCITY, TRANSVERSE NORMAL IMPACT OF A CLAMPED PLATE

Richard E. Llorens
Pennsylvania State University
Radnor Center for Graduate Studies

and

Lee W. Gause
Aircraft and Crew Systems Technology Directorate
NAVAL AIR DEVELOPMENT CENTER
Warminster, Pennsylvania 18974

5 OCTOBER 1981

FINAL REPORT
AIRTASK NO. WR0230301
Work Unit DG602

Approved for Public Release; Distribution Unlimited

Prepared for
NAVAL AIR SYSTEMS COMMAND
Department of the Navy
Washington, D. C. 20361

NOTICES

REPORT NUMBERING SYSTEM – The numbering of technical project reports issued by the Naval Air Development Center is arranged for specific identification purposes. Each number consists of the Center acronym, the calendar year in which the number was assigned, the sequence number of the report within the specific calendar year, and the official 2-digit correspondence code of the Command Office or the Functional Directorate responsible for the report. For example: Report No. NADC-78015-20 indicates the fifteenth Center report for the year 1978, and prepared by the Systems Directorate. The numerical codes are as follows:

CODE	OFFICE OR DIRECTORATE
00	Commander, Naval Air Development Center
01	Technical Director, Naval Air Development Center
02	Comptroller
10	Directorate Command Projects
20	Systems Directorate
30	Sensors & Avionics Technology Directorate
40	Communication & Navigation Technology Directorate
50	Software Computer Directorate
60	Aircraft & Crew Systems Technology Directorate
70	Planning Assessment Resources
80	Engineering Support Group

PRODUCT ENDORSEMENT – The discussion or instructions concerning commercial products herein do not constitute an endorsement by the Government nor do they convey or imply the license or right to use such products.

APPROVED BY: J. R. Woods **DATE:** 3/15/82

J. R. WOODS
CDR USN

SECURITY CLASSIFICATION OF THIS PAGE (When Data Entered)

REPORT DOCUMENTATION PAGE		READ INSTRUCTIONS BEFORE COMPLETING FORM
1. REPORT NUMBER NADC-81250-60	2. GOVT ACCESSION NO. AD-A115 760	3. RECIPIENT'S CATALOG NUMBER
4. TITLE (and Subtitle) Low Velocity, Transverse Normal Impact of a Clamped Plate		5. TYPE OF REPORT & PERIOD COVERED Final 6. PERFORMING ORG. REPORT NUMBER
7. AUTHOR(s) Richard E. Llorens Lee W. Gause		8. CONTRACT OR GRANT NUMBER(s)
9. PERFORMING ORGANIZATION NAME AND ADDRESS Aircraft & Crew Systems Technology Directorate Naval Air Development Center Warminster, PA 18974		10. PROGRAM ELEMENT, PROJECT, TASK AREA & WORK UNIT NUMBERS Airtask No. WR0230301 Work Unit DG602
11. CONTROLLING OFFICE NAME AND ADDRESS Naval Air Systems Command Department of the Navy Washington, D.C. 20361		12. REPORT DATE 5 Oct. 81 13. NUMBER OF PAGES
14. MONITORING AGENCY NAME & ADDRESS(if different from Controlling Office)		15. SECURITY CLASS. (of this report) Unclassified 15a. DECLASSIFICATION DOWNGRADING SCHEDULE

16. DISTRIBUTION STATEMENT (of this Report)

Approved for Public Release; Distribution Unlimited

17. DISTRIBUTION STATEMENT (of the abstract entered in Block 20, if different from Report)

18. SUPPLEMENTARY NOTES

19. KEY WORDS (Continue on reverse side if necessary and identify by block number)

Clamped Plate, Impact, Finite Element, Composite Materials

20. ABSTRACT (Continue on reverse side if necessary and identify by block number)

A finite element solution for the response of a clamped plate subjected to central low speed transverse impact is presented. The solution is empirically corrected, on the basis of viscoelastic beam analysis, to admit damping. Comparisons of the numerical predictions of the corrected theory with central impact test results on graphite-epoxy composite laminates show excellent agreement for two of the three test studies.

DD FORM 1 JAN 73 1473 EDITION OF 1 NOV 65 IS OBSOLETE
S/N 0102-LF-014-6601

SECURITY CLASSIFICATION OF THIS PAGE (When Data Entered)

The structural dynamic response model assumes a special orthotropic plate impacted by a rigid mass. Convenient displacement and velocity distributions are assumed as initial conditions for the finite element procedure.

TABLE OF CONTENTS

LIST OF TABLES

LIST OF FIGURES

INTRODUCTION

In the present study, we shall consider the problem of determining the ability of fiber reinforced composite material structures to sustain handling and impact loading. Such an investigation will represent an important element in assessing the applicability of such material systems for long term service utilization. Accordingly, the present work is directed toward the development of a technique which will predict the strains in clamped plates which arise as a consequence of relatively low speed (0 to 30 m/s), hard object, transverse normal impact.

Previously we have considered the problems of the low velocity impact of both beams and simply-supported orthotropic plates, i.e., references (1), (2) and (3). Thus, in reference (1) we initiated our study of low velocity impact by considering the analysis of a simply supported beam. In this first investigation it was shown that the physical problem of interest was related to the structural response of the system. Additionally, it was determined that the destruction of the beam was related to a tension failure in the extreme fiber opposite to the impact point. In reference (2) one of the authors considered the effect of the introduction of viscoelastic damping into the solution of a simply supported beam problem. Since the undamped theoretical solution tends to form an upper bound for the experimental data, this work led to an improved correlation of the theoretical and experimental data. Finally, in reference (3) one of the authors considered the extension of the undamped theory to the problem of a simply supported orthotropic plate. However, it is important to observe that this last work was extended to include damping by empirically correcting the solution according to the results of reference (2). Indeed, we may summarize the essence of all of the previous work by declaring that an undamped theoretical solution of a vibrating system suitability corrected for damping correlates the available experimental data, reference (4), to within the limits of experimental accuracy.

In view of the success of the previous investigations it was decided to extend the work to the practically important problem of a clamped plate. Since the theoretical solution of a clamped plate problem is more difficult than a corresponding simply supported plate problem and the solution of the simply supported plate, i.e., reference (3), extended over three hundred pages, a new solution technique was indicated. Thus, we considered the solution of a clamped plate subjected to impact utilizing the finite element approach. Although the present problem resides within the capacities of most general purpose finite element programs, i.e., NASTRAN, it was decided that a stand alone program which was directed at the solution of this one problem would allow a more economical parametric study of the general situation. Indeed, an initial investigation of two specific clamped plate problems employing NASTRAN required an average of thirty-three seconds of computer CPU time on the CDC computer which translated into an approximately sixty three dollar per problem charge. Certainly a large parametric study subject to such constraints would be prohibitive. NASTRAN permits the utilization of the inverse power method in the solution of the eigenvalue problem, however, it provides for no initial estimate of the magnitude of the eigenvalue. Indeed, NASTRAN avoids this problem by employing an iterative search technique which employs range estimates supplied by the user. Thus, a stand alone program which would supply initial estimates of the eigenvalues represented a desired element of the overall solution. This element of the total task was accomplished by utilizing the energy method to develop a technique which supplies approximations for the first two eigenvalues. Experimental data indicated that damping attenuated the contribution of the other mode shapes sufficiently that they were not visible in the output trace of the experimental records in the time domain under consideration. The program which resulted from this analysis produced estimates of the first and second eigenvalues which were, on the average, ten and thirty percent larger than the corresponding finite element values. Since the energy method always yields approximate values for the eigenvalues which are greater than the minimum possible value in the space under consideration, the above factors were employed to

correct the initial frequency estimates. Specifically, the first and second approximate frequencies were multiplied by factors of 0.92 and 0.76 before they were input into the finite element program. The finite element program was designed for computational efficiency and minimum storage requirements. Indeed, the program permits a ten by ten subdivision of the plate, i.e., 100 nodes, which corresponds to approximately a three hundred degrees-of-freedom finite element mode. All computational effort is performed in core with a result that for the maximum permissible subdivision of the plate the program requires only slightly over four seconds of CPU on the CDC computer. This translates into a cost of approximately three and one half dollars per problem since three problems were normally solved at one time. Finally, a third computer program was written which would accept the results of the finite element solution and determine the maximum strain at the center of the plate. This program permitted the amplitudes of the mode shapes to be corrected for damping in accord with results of the beam damping analysis, reference (2), i.e., we employed the procedure utilized in reference (3).

This report extends the analysis of composite structural impact damage by considering a boundary value problem of considerable practical utility. It is to be understood that the finite element solution coincides with the following physical problem. A mass of small dimensions, possessing unit velocity, is directed at a plate which is initially at rest. During impact the impactor transfers its momentum to the region of the plate with which it is in contact. This information is utilized to ascertain initial conditions for the vibrating system. The plate and impactor remain in contact, over a small area, during the remainder of the first quarter of the first cycle of the motion. Finally, the finite element solution is empirically corrected, on the basis of viscoelastic damped beam theory, to account for the effects of damping. Thus, the solution presented in this report considers central impact, provides the finite element approximation for the eigenvalues and eigenfunctions of a clamped plate carrying a concentrated impactor mass and it is empirically altered to account for material damping.

ANALYSIS

The work performed during this investigation may conveniently be subdivided into two distinct subsections. We shall initially describe the basis of the finite element model, then, having summarized the method of securing the eigenvalues and eigenvectors of the problem, proceed with the analysis of the impact event.

For conceptual clarity, we shall divide our description of the finite element model into two unique subtasks. First, we shall describe the finite element model and our solution of the resulting system of equations, then, we shall describe our method of approximating the eigenvalues of a vibrating clamped plate.

FINITE ELEMENT MODEL

The potential energy of a vibrating plate may be shown to be expressible in the form,

$$PE = \frac{1}{2} \int_A U(w)\, dA \qquad (1)$$

where:

A = area of plate

PE = potential energy

$$U(w) = D_{11}\, w_{xx}^2 + 2\, H\, w_{xy}^2 + D_{22}\, w_{yy}^2$$

$D_{11}, D_{22} \ldots$ = flexural rigidities of the plate

$H = D_{12} + 2D_{66}$

w = transverse displacement of the plate

Note that subscripts appended to the transverse displacement indicate partial derivatives with respect to the appropriate space variable and a dot denotes a time derivative. Further, the kinetic energy of the plate may be written as,

$$KE = \frac{1}{2} \int_A \rho h\, \dot{w}^2\, dA \tag{2}$$

where:

KE = kinetic energy

h = thickness of plate

ρ = mass density of plate

Since we are concerned with the determination of the eigenvectors, i.e., mode shapes, of the vibrating system we will assume that the motion is harmonic, or,

$$w = \overline{w} \sin \omega t \tag{3}$$

where:

$\overline{w}$ = mode shape

t = time

ω = circular frequency

Introducing the expression for the mode shape, equation (3), into the kinetic energy formula, equation (2), we find that the maximum kinetic energy, KE_{max}, is given by,

$$KE_{max} = \frac{1}{2} \omega^2 \rho h \int_A \overline{w}^2\, dA \tag{4}$$

The results expressed by equations (1) and (4) were utilized to construct a finite element representation of our problem. Details of this work are summarized in appendix A.

APPROXIMATE NATURAL FREQUENCIES

Next we turn our attention to the problem of the approximate determination of the first two natural frequencies of the system. This task is an important element of our procedure since the determination of reasonably accurate approximate frequencies will considerably reduce computational costs. Indeed, a major portion of our success in decreasing computational effort may be traced to this portion of our analysis.

In the problem under consideration we recall that the concentrated mass impacts the origin of the coordinate system and, therefore, the kinetic energy of our system may be written,

$$KE = \frac{1}{2}\tilde{M}\,\dot{w}_0^2 + \frac{1}{2}\int_A \rho h \dot{w}^2\, dA \tag{5}$$

where:

$\tilde{M}$ = mass of impacting object

$\dot{w}_0$ = velocity of the plate at the origin of the coordinate system

Introducing the expression for the mode shape, equation (3), into the potential energy expression, equation (1), and the kinetic energy expression, equation (5), and equating the resulting maximums, we obtain,

$$\omega^2 = \frac{\int_A U(\bar{w})\, dA}{\tilde{M}\,\bar{w}_0^2 + \rho h \int_A \bar{w}^2\, dA} \tag{6}$$

In order to simplify our computations we shall convert the variables under the integral sign in equation (6) to dimensionless form, i.e.,

$$\int_A \bar{w}^2\, dA = ab\int_0^1\int_0^1 \bar{w}^2\, d\zeta\, d\eta$$

$$\int_A U(\bar{w})\, dA = ab\left\{\frac{D_{11}}{a^4}\int_0^1\int_0^1 (\bar{w}_{\zeta\zeta})^2\, d\zeta\, d\eta + \frac{2D_{12}}{a^2b^2}\int_0^1\int_0^1 \bar{w}_{\zeta\zeta}\,\bar{w}_{\eta\eta}\, d\zeta\, d\eta + \right.$$

$$\left.\frac{D_{22}}{b^4}\int_0^1\int_0^1 (\bar{w}_{\eta\eta})^2\, d\zeta\, d\eta + \frac{4D_{66}}{a^2b^2}\int_0^1\int_0^1 (\bar{w}_{\zeta\eta})^2\, d\zeta\, d\eta\right\}$$

where:

a = half length of plate

b = half width of plate

$\zeta = \frac{x}{a}$

$\eta = \frac{y}{b}$

In view of the symmetry of the problem about the origin the integrations were confined to the region of the plate corresponding to positive x and y. This alteration in the integration procedure requires that we utilize one quarter of the impacting mass in equation (6).

The result indicated in equation (6) was employed to determine approximate values of the first two natural frequencies of the vibrating plate. All the details of this work are summarized in appendix B.

INVERSE POWER METHOD

Since, from the previous section, we possess approximations for the first two natural frequencies of the system it is efficient to employ an iterative procedure to solve our finite element equations. Specifically, we shall employ the computational algorithm known as the inverse power method.

After assembly the system of finite element equations is expressible in the form,

$$KX = \lambda MX \tag{7}$$

where:

K = stiffness matrix

M = mass matrix

X = eigenvector

λ = eigenvalue

We shall partition the eigenvalue λ into two parts, i.e.,

$$\lambda = \lambda_0 + \Delta\lambda$$

where:

λ_0 = approximation to the eigenvalue

$\Delta\lambda$ = correction to the approximation

Introducing the above expression for the eigenvalue into the original set of equations, equations (7), and normalizing the input vector so that the largest component assumes the value one, we obtain,

$$(K - \lambda_0 M)\, X = \Delta\lambda\, X_{max} \cdot M\left(\frac{X}{X_{max}}\right)$$

where:

X_{max} = maximum component of the solution vector

However, it may be shown that as the number of iterations increases,

$$\Delta\lambda\, X_{max} \rightarrow 1$$

Therefore, we may summarize the above analysis by defining the following algorithm,

$$(K - \lambda_0 M)\, X_{n+1} = M\left(\frac{X_n}{X_{max}}\right)$$

where:

X_n = n^{th} iteration to the eigenvector X

SOLUTION OF THE SYSTEM OF FINITE ELEMENT EQUATIONS

To reduce storage requirements and insure computational efficiency, a stand alone computer program was written employing the present analysis.

The system of equations for the finite element representation can be partitioned into a sequence of submatrices which may be expressed in the following form,

$$\begin{bmatrix} A & B^T & & & \\ B & C & D^T & & \\ & D & C & D^T & \\ & & \ddots & \ddots & \ddots \\ & & & D & C \end{bmatrix} \begin{Bmatrix} X_1 \\ X_2 \\ X_3 \\ \vdots \\ X_L \end{Bmatrix} = \begin{Bmatrix} R_1 \\ R_2 \\ R_3 \\ \vdots \\ R_L \end{Bmatrix}$$

where:

A, B, C and D are constant submatrices

$R_1, R_2, \ldots R_L$ given column vectors

$X_1, \ldots X_L$ unknown column vectors

We shall adopt a solution procedure which removes the subarrays which lie below the main diagonal. Further, the technique shall yield submatrices which are symmetric along the main diagonal.

Let us consider the solution of the following set of equations, i.e.,

$$S_i X_i + D^T X_{i+1} = \tilde{R}_i$$

$$D X_i + C X_{i+1} + D^T X_{i+2} = R_{i+1}$$

where:

$\tilde{R}_i$ = column vector which will be defined later.

S_i = symmetric matrix which will be defined later.

Multiplying the first set of equations by DS_i^{-1} and subtracting the result from the second set, we obtain the following equivalent set of equations,

$$S_i X_i + D^T X_{i+1} = \tilde{R}_i$$

$$0 X_i + (C - DS_i^{-1} D^T) X_{i+1} + D^T X_{i+2} = R_{i+1} - DS_i^{-1} \tilde{R}_i$$

Since matrices S_i and C are symmetric it may be shown that the matrix $C - DS_i^{-1} D^T$ is symmetric. Starting with the initial set of equations, the above procedure may be employed to remove those arrays which lie below the main diagonal. Continuing this process to the last set of equations, we obtain,

$$(C - DS_{L-1}^{-1} D^T) X_L = R_L - DS_{L-1}^{-1} \tilde{R}_{L-1}$$

In view of the previous work, we have replaced our original problem by that of determining a solution of the following set of equivalent equations, i.e.,

$$AX_1 + B^T X_2 = R_1$$

$$S_i X_i + D^T X_{i+1} = \tilde{R}_i, \; i = 2, \ldots, L-1$$

$$S_L X_L = \tilde{R}_L$$

where:

$$S_2 = C - BA^{-1} B^T$$

$$S_i = C - DS_{i-1}^{-1} D^T, \; i \geq 3$$

$$\tilde{R}_1 = R_1$$

$$\tilde{R}_2 = R_2 - BA^{-1} \tilde{R}_1$$

$$\tilde{R}_i = R_i - DS_{i-1}^{-1} \tilde{R}_{i-1}, \; i \geq 3$$

Utilizing the method of back substitution, i.e., starting with the last of the previous set of equations, we may write the solution of these equations in the form,

$$X_L = S_L^{-1} \tilde{R}_L$$

$$X_i = S_i^{-1} (\tilde{R}_i - D^T X_{i+1}), \; L > i > 1$$

$$X_1 = A^{-1} (R_1 - B^T X_2)$$

It is of some importance to observe that only the inverse of the S matrices need be stored in the computer. Further, since these matrices are symmetric only slightly more than half the elements of these arrays need be placed in core. Finally, the process of back substitution is to be performed in the order indicated by the brackets, i.e., only vector products are employed in the computations.

REPRESENTATION OF THE PHYSICAL SYSTEM

Since we have completed our discussion of the finite element model we may consider the problem of obtaining a mathematical representation of the physical system.

To ascertain the motion of the vibrating system we shall neglect damping and assume a normal expansion, i.e.,

$$w(x, y, t) = \sum_{i=1}^{\infty} a_i \overline{w}_i (x, y) \sin \omega_i t \tag{8}$$

where:

a_i = magnitude of normalized mode

$\overline{w}_i (x, y) = i^{th}$ mode shape.

Differentiating the previous expression, equation (8), with respect to t and evaluating the result at t = 0, we determine that,

$$\frac{\partial w}{\partial t} (x, y, o) = \sum_{i=1}^{\infty} \omega_i a_i \overline{w}_i (x, y)$$

Multiplying this last result by $\overline{w}_j \rho h dx dy$ and integrating over the surface of the plate, we obtain after algebraic reduction,

$$\frac{\widetilde{M}}{4\rho h} \overline{w}_j (o, o) \frac{\partial w}{\partial t} (o, o, o) + \int_0^a \int_0^b \overline{w}_j \frac{\partial w}{\partial t} (x, y, o)\, dx\, dy =$$

$$\sum_{i=1}^{\infty} \omega_i a_i \left\{ \frac{\widetilde{M}}{4\rho h} \overline{w}_j (o, o) \overline{w}_i (o, o) + \int_0^a \int_0^b \overline{w}_j \overline{w}_i\, dx\, dy \right\} \tag{9}$$

Recalling that the initial impact event is constrained to a neighborhood of the origin, we may write,

$$\int_0^a \int_0^b \overline{w}_j \frac{\partial w}{\partial t} (x, y, o)\, dx\, dy \cong \epsilon_1 \epsilon_2 \overline{w}_j (o, o) \frac{\partial w}{\partial t} (o, o, o)$$

where:

ϵ_1, ϵ_2 = half of the length and width of the impact zone, respectively.

Since linear theory implies the output response varies linearly with velocity we consider the plate response corresponding to a unit velocity. Therefore, utilizing a unit velocity in the conservation of momentum equation, we have,

$$\widetilde{M} \cdot 1 = \left\{ \widetilde{M} + 4\rho h \epsilon_1 \epsilon_2 \right\} \frac{\partial w}{\partial t} (o, o, o)$$

Substituting the last two results into equation (9) we discover that,

$$\sum_{i=1}^{\infty} \omega_i a_i \left\{ \frac{\tilde{M}}{4\rho h} \overline{w_j}(o,o)\,\overline{w_i}(o,o) + \int_0^a \int_0^b \overline{w_j}\,\overline{w_i}\,dx\,dy \right\} = \frac{\tilde{M}}{4\rho h}\overline{w_j}(o,o)$$

Utilizing the orthogonality relations between the modes, we conclude that,

$$a_i = \frac{\frac{\tilde{M}}{4\rho h}\overline{w_i}(o,o)}{\omega_i \left\{ \frac{\tilde{M}}{4\rho h}\overline{w_i}^2(o,o) + \int_0^a \int_0^b \overline{w_i}^2\,dx\,dy \right\}} \tag{10}$$

Observe that equation (10) implies that to ascertain the amplitude of a specific mode we must possess the value of the integral of the square of the displacement of the corresponding mode. To obtain this quantity, a numerical approximation to the integration was performed in the computer program. Such work is summarized in appendix C.

Finally, equation (8) was empirically altered in accord with the results of beam theory, by the inclusion in each mode of an exponential damping factor, i.e.,

$$w(x,y,t) = \sum_{i=1}^{\infty} a_i \overline{w_i}(x,y)\, e^{-0.5K\omega_i^2 t} \sin \omega_i t \tag{11}$$

where:

K = damping constant

Equation (11) served as the model by which the other functions of displacement, i.e., strain, were similarly modified.

Work performed during the analysis phase led to the creation of three distinct programs. First, a computer program was developed which generated initial estimates of the first two natural frequencies of a clamped plate. Generally, the approximation procedure yielded first frequencies which were approximately ten percent too large and second frequencies which were thirty percent too great. Specifically, it was necessary to multiply the first approximate frequencies by 0.92 and the second approximate frequencies by 0.76 before introducing these values into the second program. These factors are not exact and could change with the application, indeed, their only purpose is to improve the rate of convergence of the second program. Finally, we observe that the program requires little CPU time on the CDC computer to accomplish its objectives.

Next a computer program was developed to perform the analysis indicated by the finite element model. This program utilized both the bending element and the solution technique outlined previously in this paper. The program admits a 10 by 10 node subdivision of the plate and since there are three degrees-of-freedom per node the program formulates a model of slightly less than three hundred equations with a corresponding set of unknowns. Finally, we note that the program required a maximum of slightly more than four seconds of CPU time on the CDC computer for a single problem as compared to an approximate thirty three second CPU time on the CDC computer for a NASTRAN solution of the corresponding problem.

The last computer program utilized some of the results of the second computer program to predict the maximum strain in the plate. Values of damping corresponding to those adopted in the simply supported plate analysis were employed in the present work. Again we observe that the program required minimal CPU time on the CDC computer to perform its calculations.

CONCLUSIONS

All three programs were utilized to predict the response of the clamped plates tested by Chou and Flis in reference (4). No difficulties were experienced in the operation of the programs and the results of this work are summarized in figures 1 to 16 and tables I, II and III.

Comparison of the B-series experimental results and the theoretical calculations indicate fundamental differences between the analysis and this data. Unfortunately, the experimental results lie above the theoretical curve corresponding to the case of no damping. At no time during any of our previous analysis of beams and plates did a set of experimental data exceed the "no damping" computations. Thus, it is difficult to reach a practical conclusion at the present time. Either the theoretical model does not correspond to the physical experiments, i.e., rebound of the impactor before the maximum strain occurs, or the experimental tests are much more subtle than one would normally expect. The experimental points parallel the "no damping" computations indicating a linear analysis of the data is correct and, in addition, the ϵ_{xx}/v and ϵ_{yy}/v data points from the same strain gage occupy the same position relative to the several damping curves. Thus, there is an apparent intrinsic consistency between the experimental and theoretical data.

In the case of the F and H-series data, the situation is considerably different. Most of the data is found to be scattered between the theoretical curves corresponding to damping values of 25×10^{-6} and 100×10^{-6}. Thus, these two sets of data exhibit approximately the same order of damping as we discovered for the simply supported plates, i.e., reference (3). Since the identical plates were employed for the two different sets of tests it appears that the boundary conditions do not seriously alter the value of the damping constant. Therefore, it would appear that the empirical damping correction is sufficient to correlate both the simply supported and clamped plates and the damping constants are not greatly affected by the variation in the boundary conditions. Finally, we may record that the experimental points exhibit the theoretical trends, indicating a linear analysis is valid and, further, the ϵ_{xx}/v and ϵ_{yy}/v experimental data for the same gage occupies the same position relative to the theoretical curves so that the data appears to be internally consistent.

Table I – Physical Configuration of Graphite/Epoxy Plates Impact Tested in Reference 4

Series Designation and Stacking Sequence	Plate Designation	Dimensions, a x b x h (mm)	Mass (Kg)
Basic lay-up (B-series) $[(\pm 45/0_2)_2/\pm 45/0/90]_s$	B1	133 x 133 x 3.6	0.099
	B2	133 x 260 x 3.6	0.193
	B3	260 x 133 x 3.6	0.193
	B4	260 x 260 x 3.6	0.379
	B5	133 x 387 x 3.6	0.287
	B6	387 x 133 x 3.6	0.287
	B7	387 x 260 x 3.6	0.547
	B8	260 x 387 x 3.6	0.547
	B9	387 x 387 x 3.6	0.815
F-series $[(\pm 45/0_2)_2/\pm 45/0/90]_{2s}$	F1	133 x 133 x 7.6	0.237
	F2	133 x 260 x 7.6	0.452
	F3	260 x 133 x 7.6	0.452
	F4	260 x 260 x 7.6	0.860
H-series $[+45/90/-45/+22.5/-67.5/-22.5/+67.5/\pm 45/+67.5/+22.5/-67.5/-22.5/\pm 67.5/\pm 22.5/0_2/\pm 22.5]_s$	H1	133 x 133 x 6.8	0.213
	H2	133 x 260 x 6.8	0.410
	H3	260 x 133 x 6.8	0.410
	H4	260 x 260 x 6.8	0.772

Table II — Experimental and Theoretical Values of the Strain/Unit Velocity for B Plate Series

	Impactor Mass, Kg	Velocity, M/sec	ϵ xx/V x 10^{+3}, sec/M				ϵ yy/V x 10^{+3}, sec/M			
			Exp.	K, Damping Constant			Exp.	K, Damping Constant		
				0	25 x 10^{-6}	100 x 10^{-6}		0	25 x 10^{-6}	100 x 10^{-6}
B1	0.228	1.73	1.39	1.80	1.46	1.24	1.97	2.62	2.03	1.72
		2.45	1.40				2.04			
		2.99	1.39				1.84			
	0.453	1.73	1.88	2.48	2.14	1.90	2.72	3.57	2.99	2.66
		2.45	1.95				2.85			
		2.99	2.01				2.93			
	0.907	1.73	2.75	3.47	3.11	2.85	3.82	4.97	4.35	3.99
B2	0.228	1.73	1.42	1.30	1.21	1.03	2.15	1.67	1.50	1.26
		2.45	1.53				2.13			
		2.99	1.48				2.11			
	0.453	1.73	2.05	1.84	1.76	1.58	2.80	2.33	2.19	1.96
		2.45	2.06				2.80			
		2.99	2.12				2.89			
	0.907	1.73	2.95	2.68	2.57	2.37	3.93	3.41	3.21	2.95
B3	0.228	1.73	1.26	1.09	0.90	0.75	2.14	1.77	1.56	1.33
		2.45	1.14				2.29			
		2.99	1.42				2.41			
	0.453	1.73	1.33	1.50	1.28	1.17	2.78	2.47	2.24	2.05
		2.45	1.39				2.76			
		2.99	1.20				2.41			
	0.907	1.73	1.97	2.09	1.87	1.76	4.13	3.48	3.27	3.07
		2.45	1.88				4.00			
B4	0.228	1.73	0.93	0.92	0.79	0.63	1.38	1.38	1.14	0.87
		2.45	0.92				1.31			
		2.99	0.99				1.35			
	0.453	1.73	1.39	1.26	1.12	0.97	1.99	1.86	1.61	1.35
		2.45	1.35				1.88			
		2.99	1.40				1.82			
	0.907	1.73	1.89	1.84	1.63	1.49	2.37	2.68	2.31	2.07

Table II – Experimental and Theoretical Values of the Strain/Unit Velocity for B Plate Series (Continued)

	Impactor Mass, Kg	Velocity, M/sec	$\epsilon xx/V \times 10^{+3}$, sec/M				$\epsilon yy/V \times 10^{+3}$, sec/M			
			Exp.	K, Damping Constant			Exp.	K, Damping Constant		
				0	25×10^{-6}	100×10^{-6}		0	25×10^{-6}	100×10^{-6}
B5	0.228	1.73	1.43	1.22	1.16	0.99	1.73	1.31	1.24	1.07
		2.45	1.43				1.71			
		2.99	1.41				1.81			
	0.453	1.73	2.02	1.79	1.71	1.53	2.60	1.97	1.87	1.66
		2.45	2.06				2.63			
		2.99	2.21				2.94			
	0.907	1.73	3.06	2.63	2.48	2.29	3.96	2.90	2.71	2.50
B6	0.228	1.73	1.16	0.79	0.73	0.63	1.75	1.56	1.48	1.31
		2.45	1.10				1.86			
		2.99	1.08				1.84			
	0.453	1.73	1.78	1.22	1.13	1.00	2.92	2.44	2.32	2.10
		2.45	1.63				2.92			
		2.99	1.54				2.72			
	0.907	1.73	2.23	1.67	1.59	1.51	4.08	3.29	3.23	3.05
B7	0.228	1.73	0.58	0.71	0.59	0.44	1.04	1.08	0.93	0.71
		2.45	0.57				0.98			
		2.99	0.64				1.00			
	0.453	1.73	1.07	1.01	0.89	0.71	1.59	1.56	1.40	1.16
		2.45	1.04				1.57			
		2.99	1.02				1.57			
	0.907	1.73	1.42	1.36	1.18	1.04	2.40	2.13	1.89	1.70
		2.45	1.39				2.47			
B8	0.228	1.73	0.46	0.55	0.54	0.51	0.93	0.68	0.65	0.59
		2.45	0.45				0.96			
		2.99	0.47				1.00			
	0.453	1.73	0.84	1.02	0.97	0.88	1.62	1.37	1.27	1.11
		2.45	0.84				1.57			
		2.99	0.90				1.57			
	0.907	1.73	1.33	1.49	1.44	1.35	2.51	1.98	1.88	1.70
		2.45	1.31				2.45			

Table III – Experimental and Theoretical Values of the Strain/Unit Velocity for F Plate Series

	Impactor Mass, Kg	Velocity, M/sec	ϵ xx/V x 10^{+3}, sec/M				ϵ yy/V x 10^{+3}, sec/M			
			Exp.	K, Damping Constant			Exp.	K, Damping Constant		
				0	25 x 10^{-6}	100 x 10^{-6}		0	25 x 10^{-6}	100 x 10^{-6}
F1	0.228	1.73	0.66	1.35	0.95	0.64	0.94	1.95	1.29	0.67
		2.45	0.68				0.95			
		2.99	0.67				0.98			
	0.453	1.73	0.88	1.94	1.47	1.09	1.33	2.77	2.01	1.49
		2.45	0.91				1.35			
		2.99	0.92				1.39			
	0.907	1.73	1.17	2.67	2.21	1.76	1.79	3.77	3.03	2.42
		2.45	1.22				1.84			
F2	0.228	1.73	0.56	0.85	0.76	0.53	0.72	0.99	0.89	0.63
		2.45	0.55				0.73			
		2.99	0.53				0.74			
	0.453	1.73	0.82	1.38	1.21	0.91	1.11	1.74	1.47	1.10
		2.45	0.82				1.12			
		2.99	0.82				1.13			
	0.907	1.73	1.21	1.98	1.83	1.47	1.72	2.48	2.23	1.80
		2.45	1.19				1.71			
F3	0.228	1.73	0.43	0.80	0.55	0.40	0.72	1.24	0.96	0.72
		2.45	0.47				0.75			
		2.99	0.44				0.72			
	0.453	1.73	0.72	1.18	0.89	0.69	1.27	1.87	1.54	1.20
		2.45	0.69				1.25			
		2.99	0.74				1.22			
	0.907	1.73	0.93	1.60	1.34	1.13	1.68	2.58	2.30	1.94
		2.45	0.90				1.67			

Table III – Experimental and Theoretical Values of the Strain/Unit Velocity for F Plate Series (Continued)

	Impactor Mass, Kg	Velocity, M/sec	$\epsilon xx/V \times 10^{+3}$, sec/M				$\epsilon yy/V \times 10^{+3}$, sec/M			
			Exp.	K, Damping Constant			Exp.	K, Damping Constant		
				0	25×10^{-6}	100×10^{-6}		0	25×10^{-6}	100×10^{-6}
F4	0.228	1.73	0.46	0.62	0.43	0.32	0.72	0.94	0.59	0.42
		2.45	0.47				0.73			
		2.99	0.49				0.74			
	0.453	1.73	0.72	0.99	0.75	0.58	1.01	1.46	1.05	0.79
		2.45	0.69				0.96			
		2.99	0.67				0.92			
	0.907	1.73	1.07	1.37	1.12	0.97	1.56	1.98	1.56	1.32
		2.45	1.02				1.50			

Table IV – Experimental and Theoretical Values of the Strain/Unit Velocity for H Plate Series

	Impactor Mass, Kg	Velocity, M/sec	$\epsilon xx/V \times 10^{+3}$, sec/M			$\epsilon yy/V \times 10^{+3}$, sec/M			
			Exp.	K, Damping Constant			Exp.	K, Damping Constant		
				0	25×10^{-6}	100×10^{-6}		0	25×10^{-6}	100×10^{-6}
H1	0.228	1.73	0.98	1.59	1.09	0.75	0.82	1.41	0.99	0.68
		2.45	0.95				0.82			
		2.99	1.00				0.81			
	0.453	1.73	1.32	2.32	1.69	1.27	1.16	2.07	1.53	1.15
		2.45	1.34				1.10			
		2.99	1.35				1.10			
	0.907	1.73	1.75	3.19	2.53	2.05	1.49	2.85	2.29	1.86
		2.45	1.80				1.63			
H2	0.228	1.73	0.76	1.02	0.85	0.62	0.61	0.82	0.61	0.45
		2.45	0.81				0.62			
		2.99	0.82				0.62			
	0.453	1.73	1.39	1.58	1.35	1.05	1.07	1.25	1.00	0.77
		2.45	1.42				1.10			
		2.99	1.46				1.14			
	0.907	1.73	1.95	2.15	2.01	1.68	1.50	1.68	1.49	1.25
		2.45	2.04				1.52			
H3	0.228	1.73	0.61	0.88	0.72	0.52	0.64	0.90	0.79	0.57
		2.45	0.62				0.68			
		2.99	0.68				0.74			
	0.453	1.73	1.19	1.43	1.18	0.90	1.28	1.44	1.25	0.96
		2.45	1.22				1.29			
		2.99	1.25				1.32			
	0.907	1.73	1.73	1.92	1.76	1.46	1.81	1.97	1.86	1.54
		2.45	1.76				1.85			

Table IV – Experimental and Theoretical Values of the Strain/Unit Velocity for H Plate Series (Continued)

	Impactor Mass, Kg	Velocity, M/sec	$\epsilon xx/V \times 10^{+3}$, sec/M			$\epsilon yy/V \times 10^{+3}$, sec/M			
			Exp.	K, Damping Constant			Exp.	K, Damping Constant	
				0	25×10^{-6}	100×10^{-6}		0	25×10^{-6}	100×10^{-6}
H4	0.228	1.73	0.69	0.85	0.54	0.38	0.58	0.75	0.48	0.34
		2.45	0.65				0.56			
		2.99	0.66				0.58			
	0.453	1.73	0.71	1.24	0.89	0.68	0.64	1.10	0.80	0.62
		2.45	0.69				0.55			
		2.99	0.72				0.55			
	0.907	1.73	1.17	1.61	1.26	1.12	0.80	1.43	1.13	1.01
		2.45	1.29				1.14			

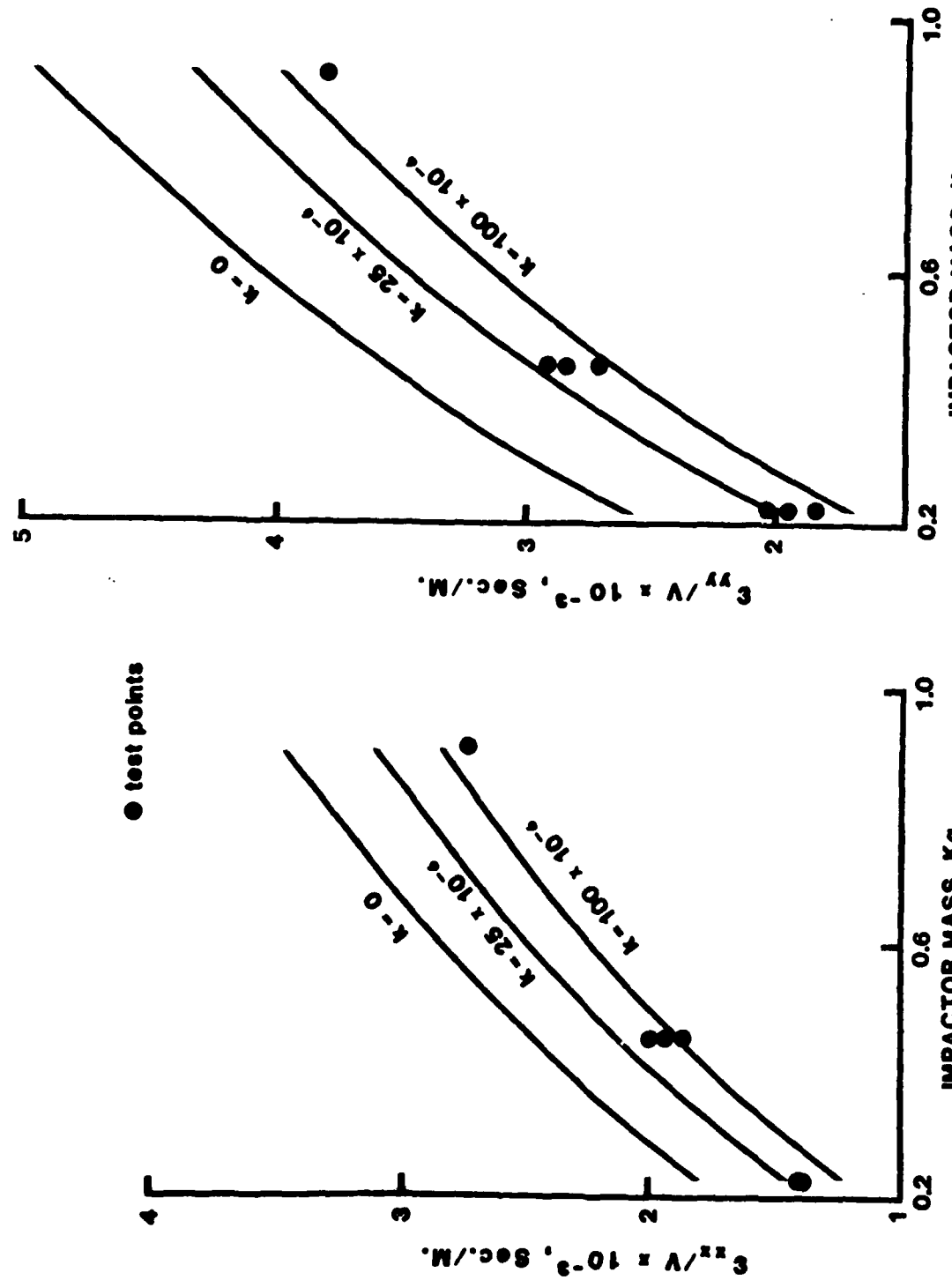

* ε_{xx}/v represents the strain in the x-direction per unit velocity

** ε_{yy}/v represents the strain in the y-direction per unit velocity

Note: Physical configuration and parametric values for each of the plate series may be found in reference (4).

Figure 1 – Comparison Between Theoretical and Experimental Results for Plate B1

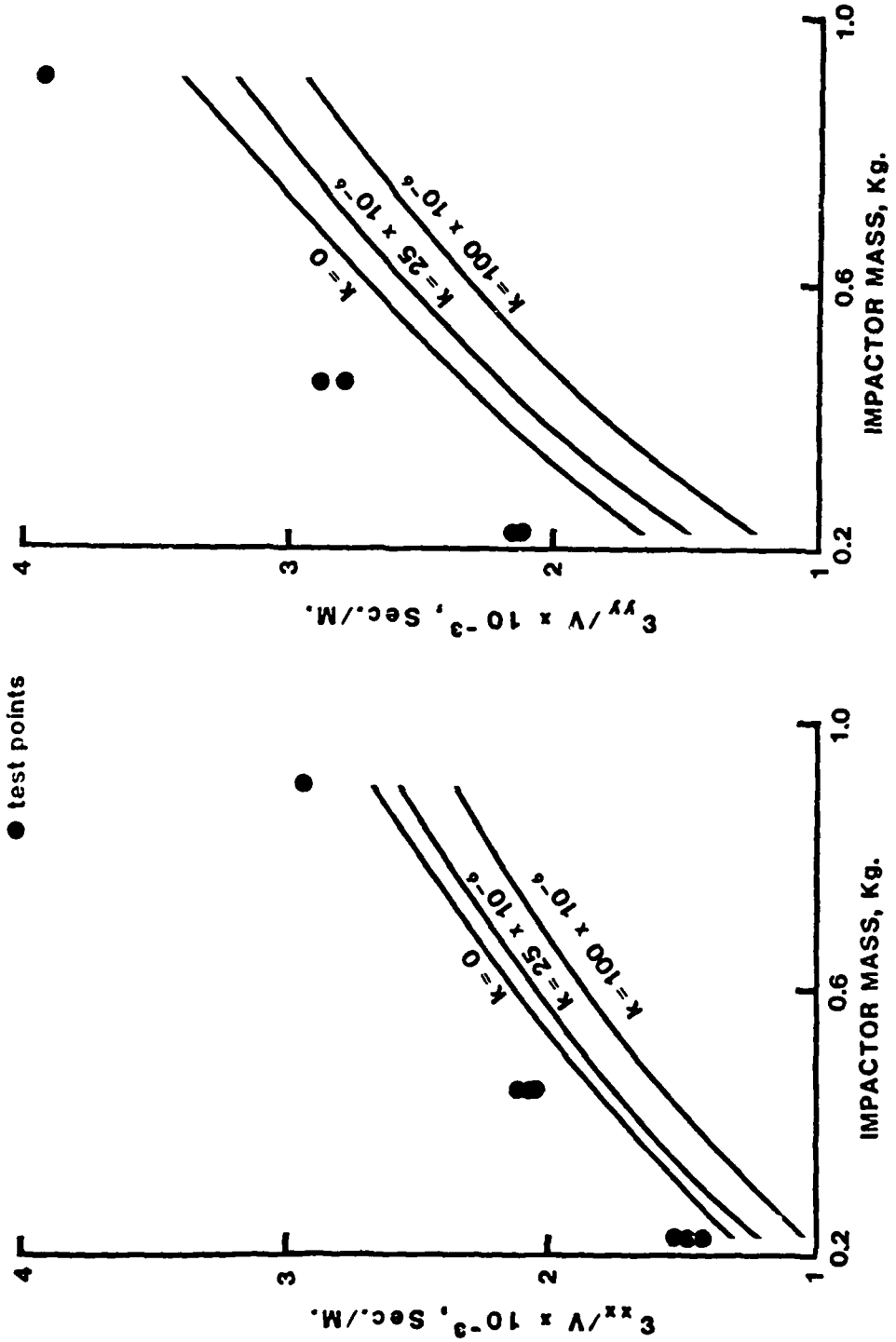

Figure 2 — Comparison Between Theoretical and Experimental Results for Plate B2

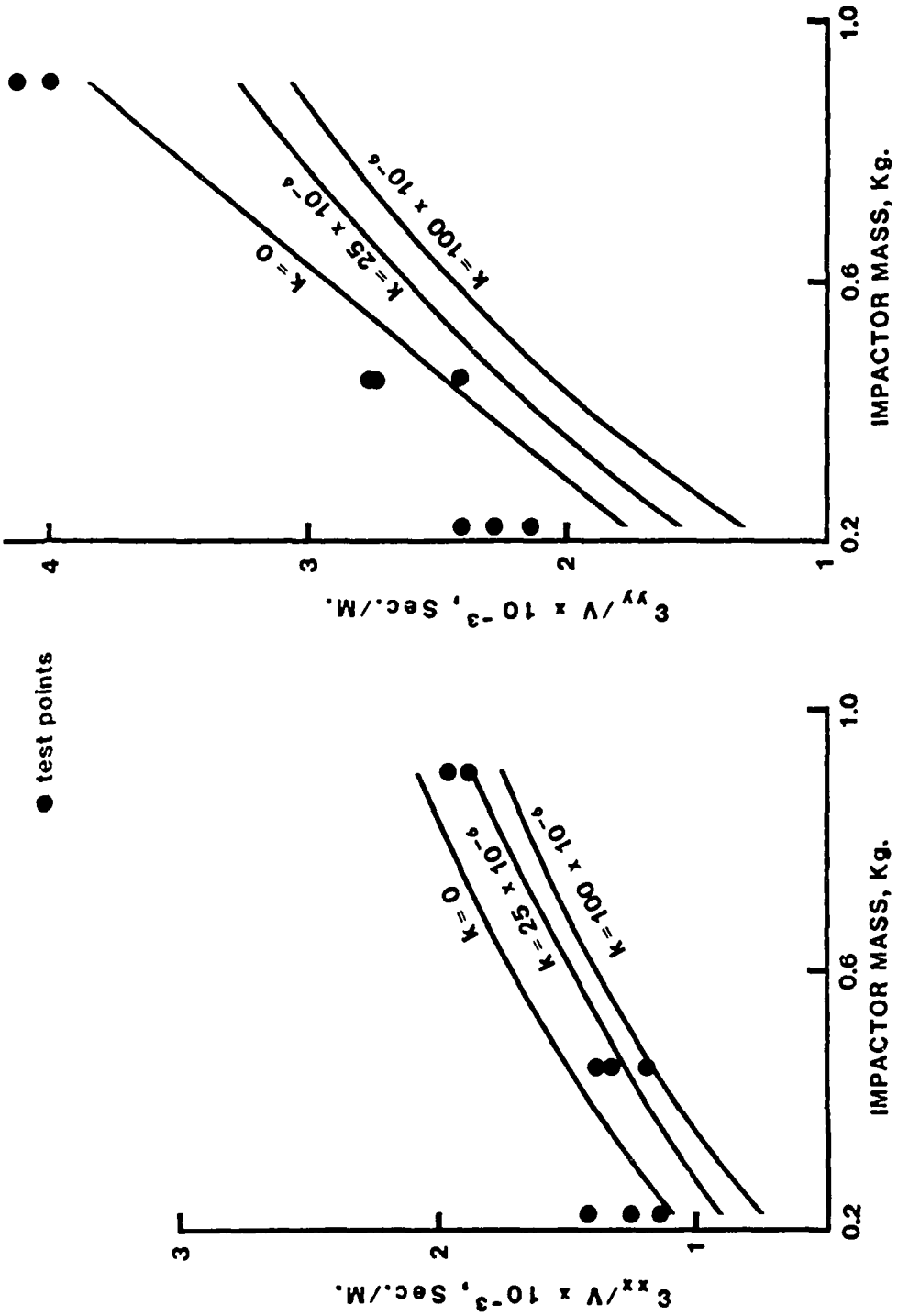

Figure 3 — Comparison Between Theoretical and Experimental Results for Plate B3

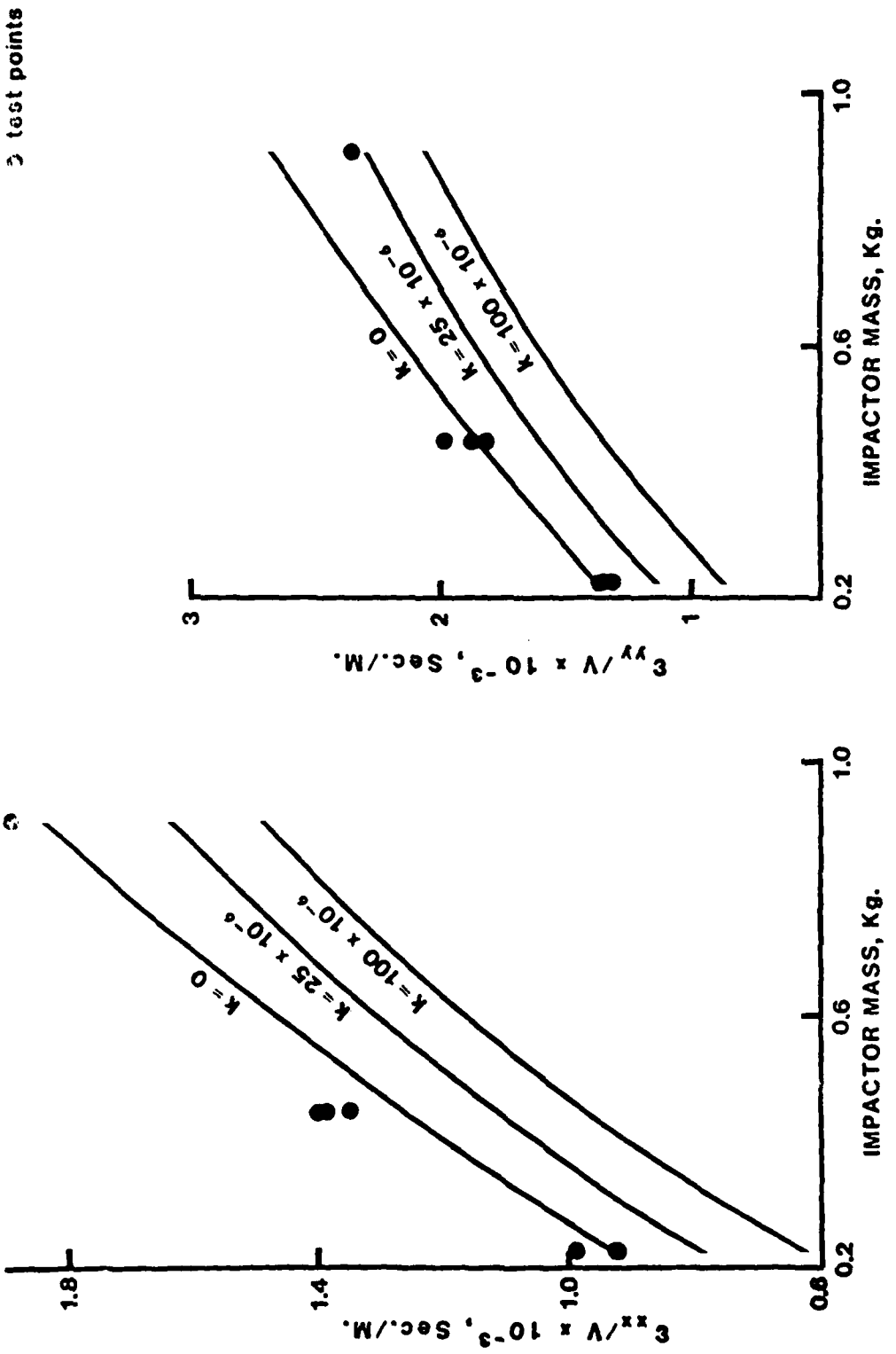

Figure 4 – Comparison Between Theoretical and Experimental Results for Plate B4

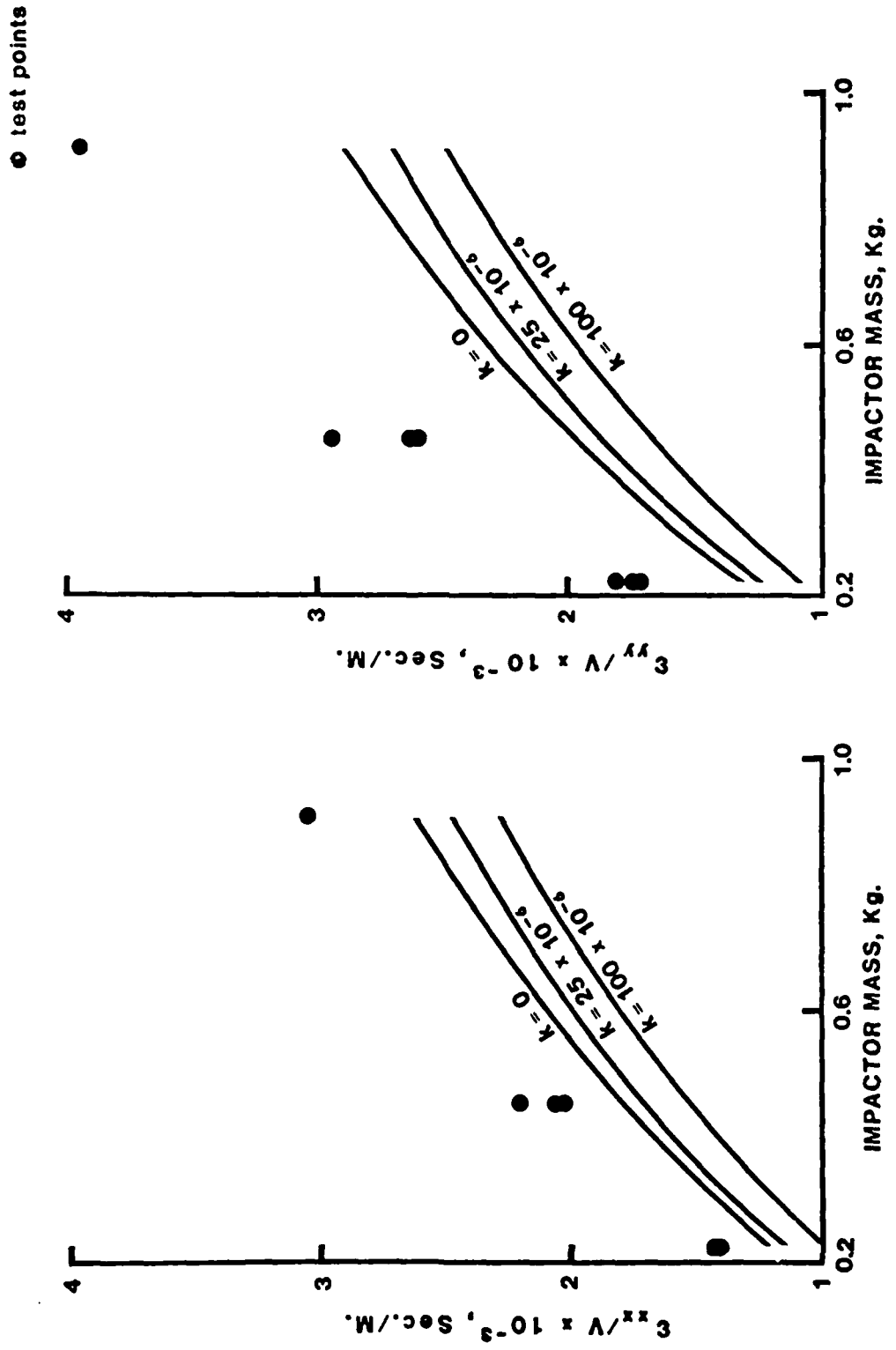

Figure 5 – Comparison Between Theoretical and Experimental Results for Plate B5

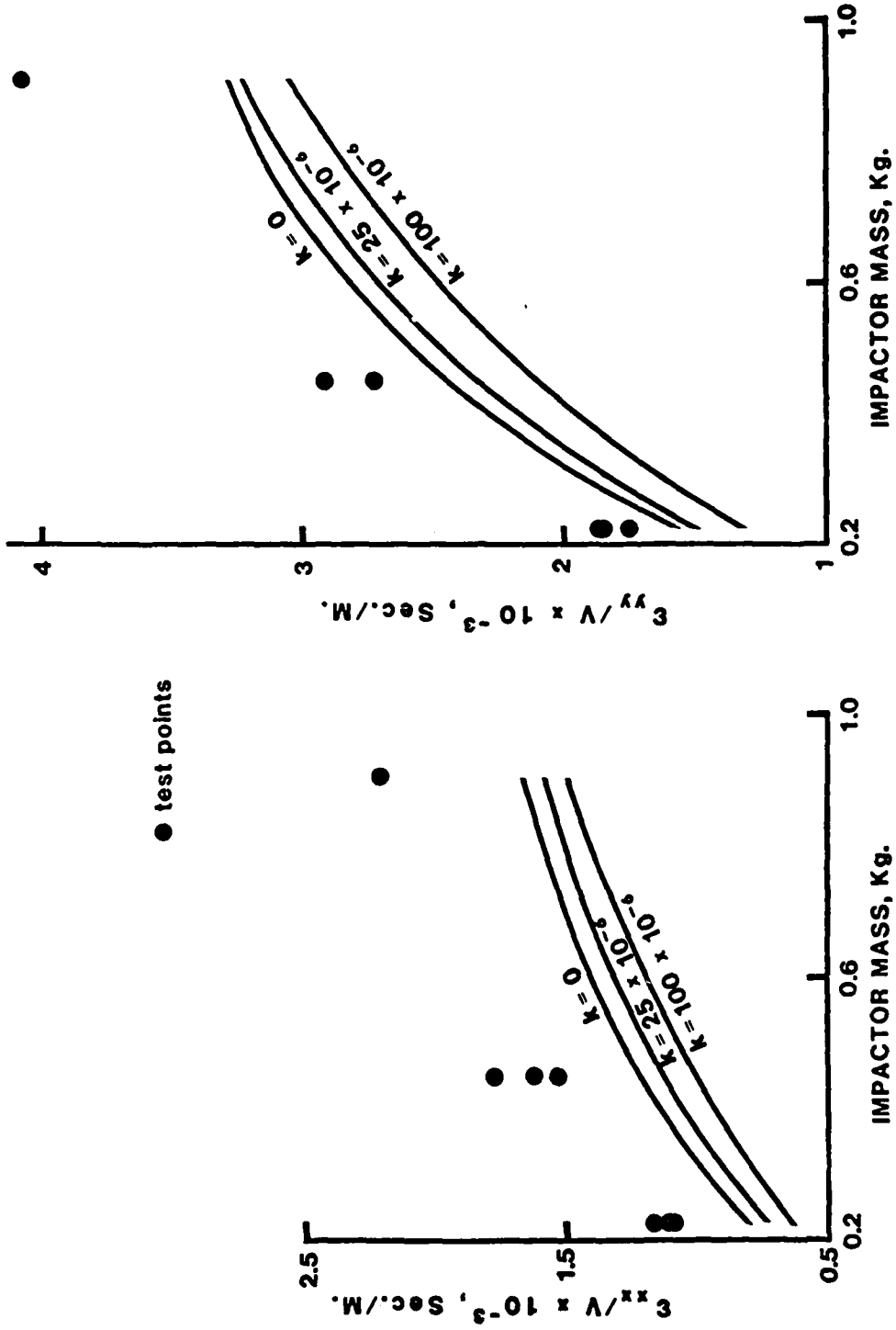

Figure 6 – Comparison Between Theoretical and Experimental Results for Plate B6

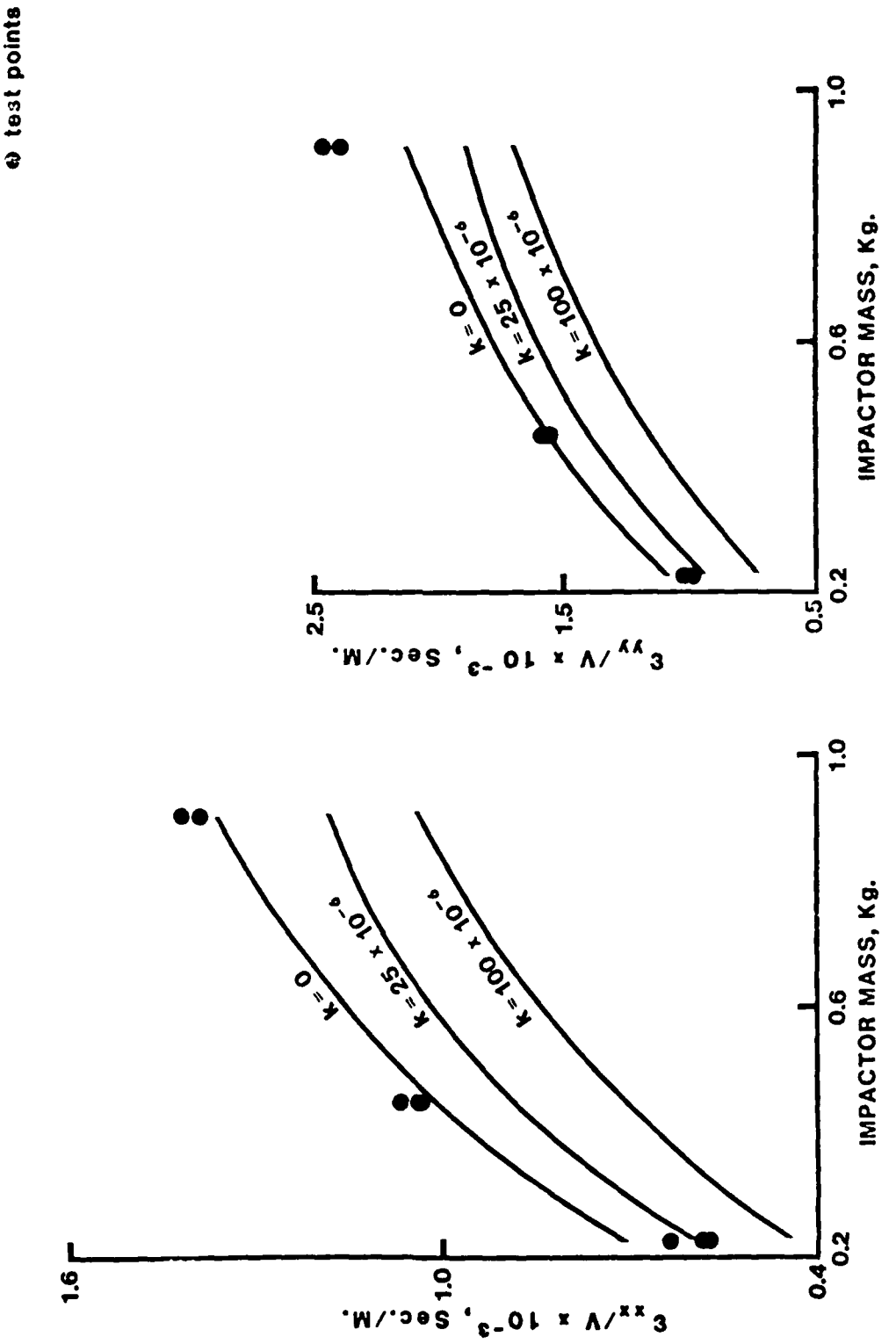

Figure 7 — Comparison Between Theoretical and Experimental Results for Plate B7

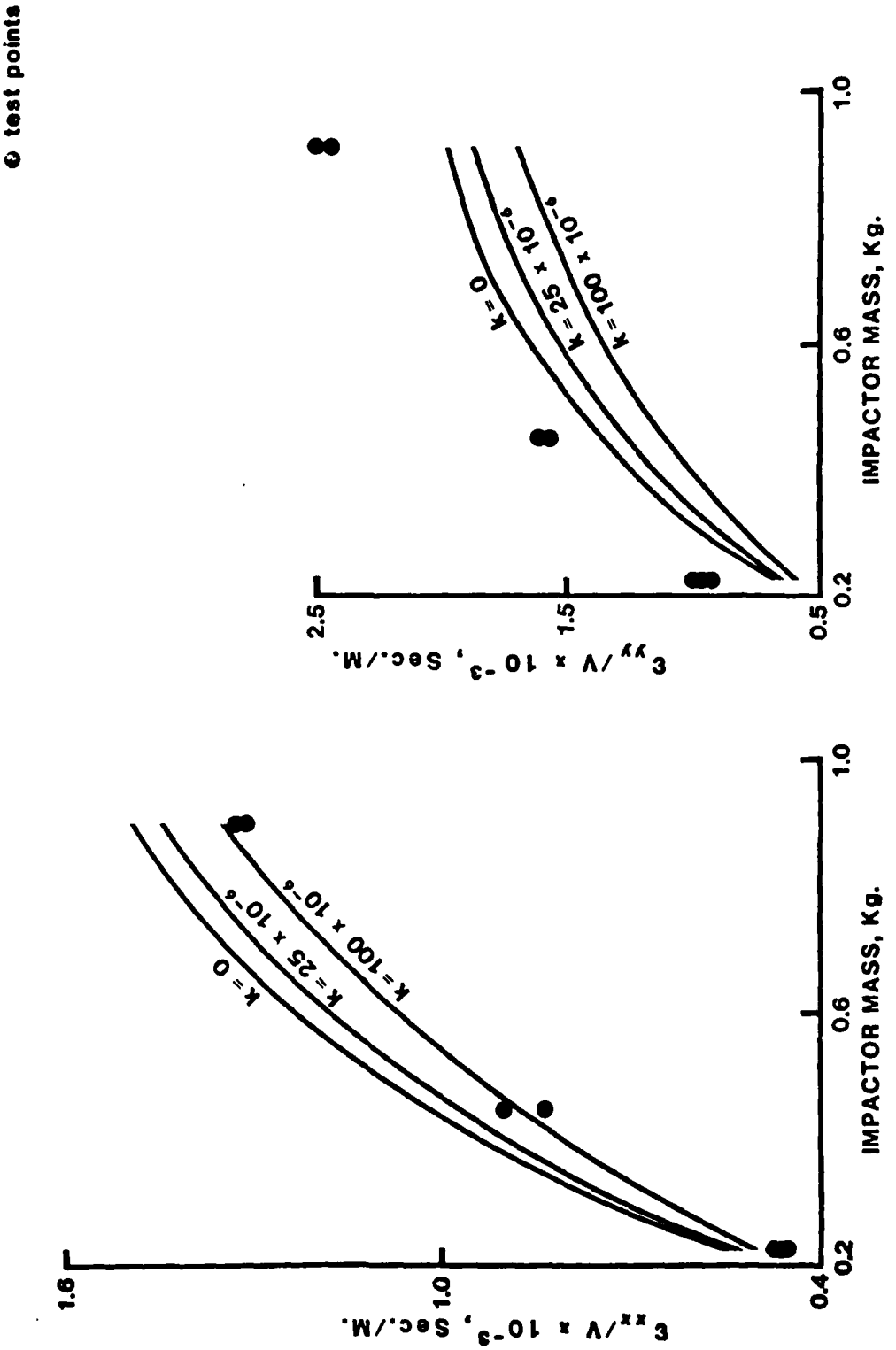

Figure 8 – Comparison Between Theoretical and Experimental Results for Plate B8

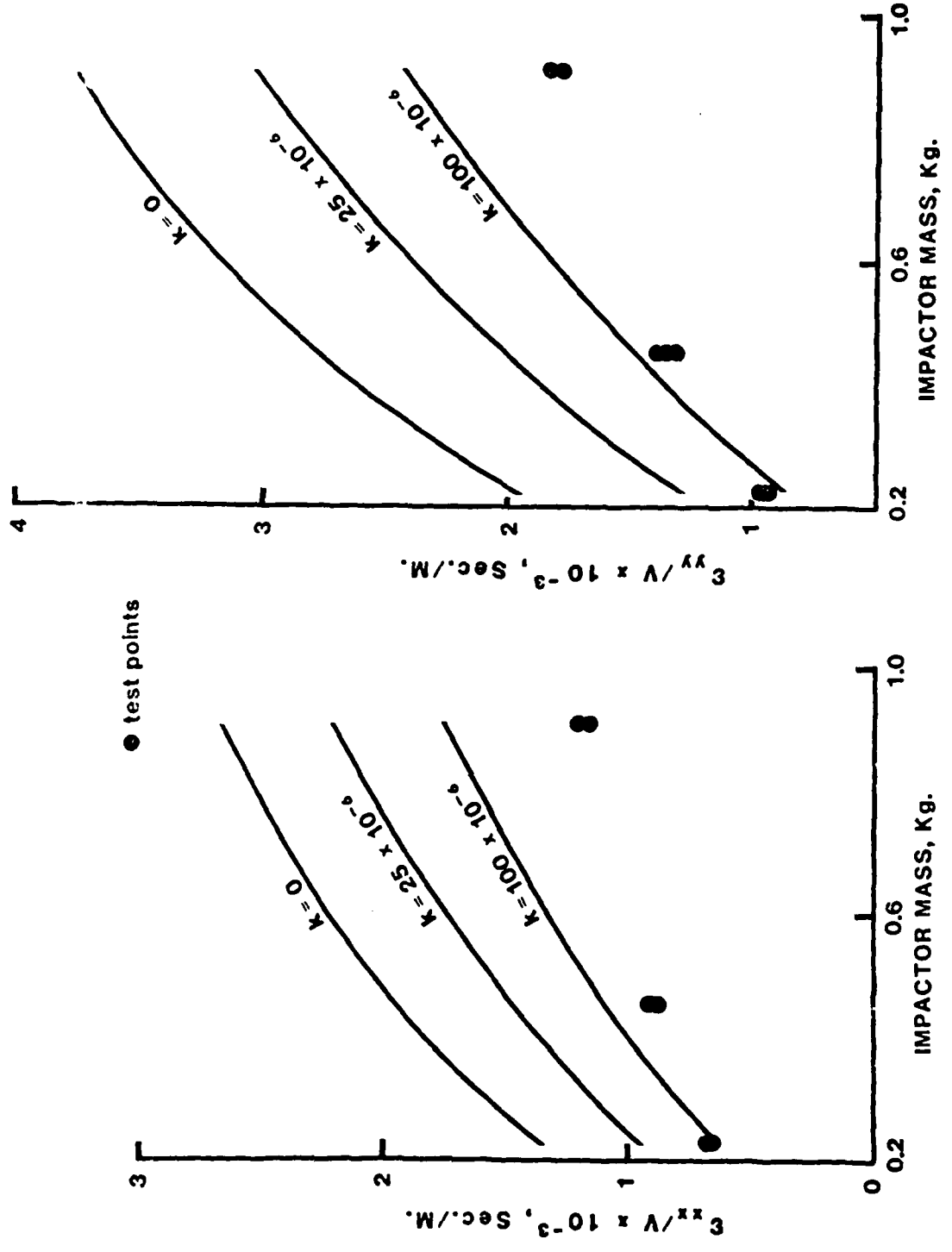

Figure 9 – Comparison Between Theoretical and Experimental Results for Plate F1

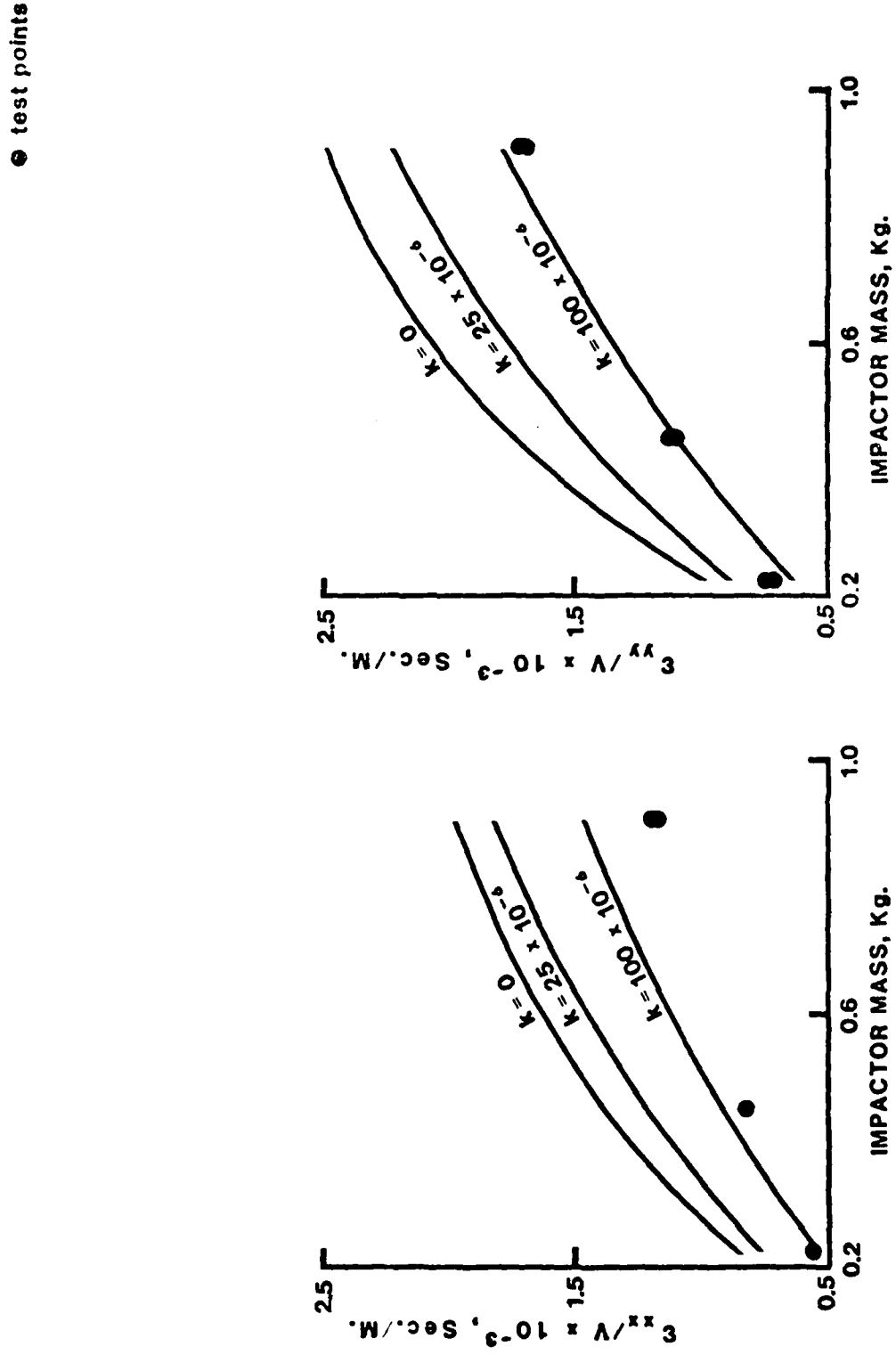

Figure 10 -- Comparison Between Theoretical and Experimental Results for Plate F2

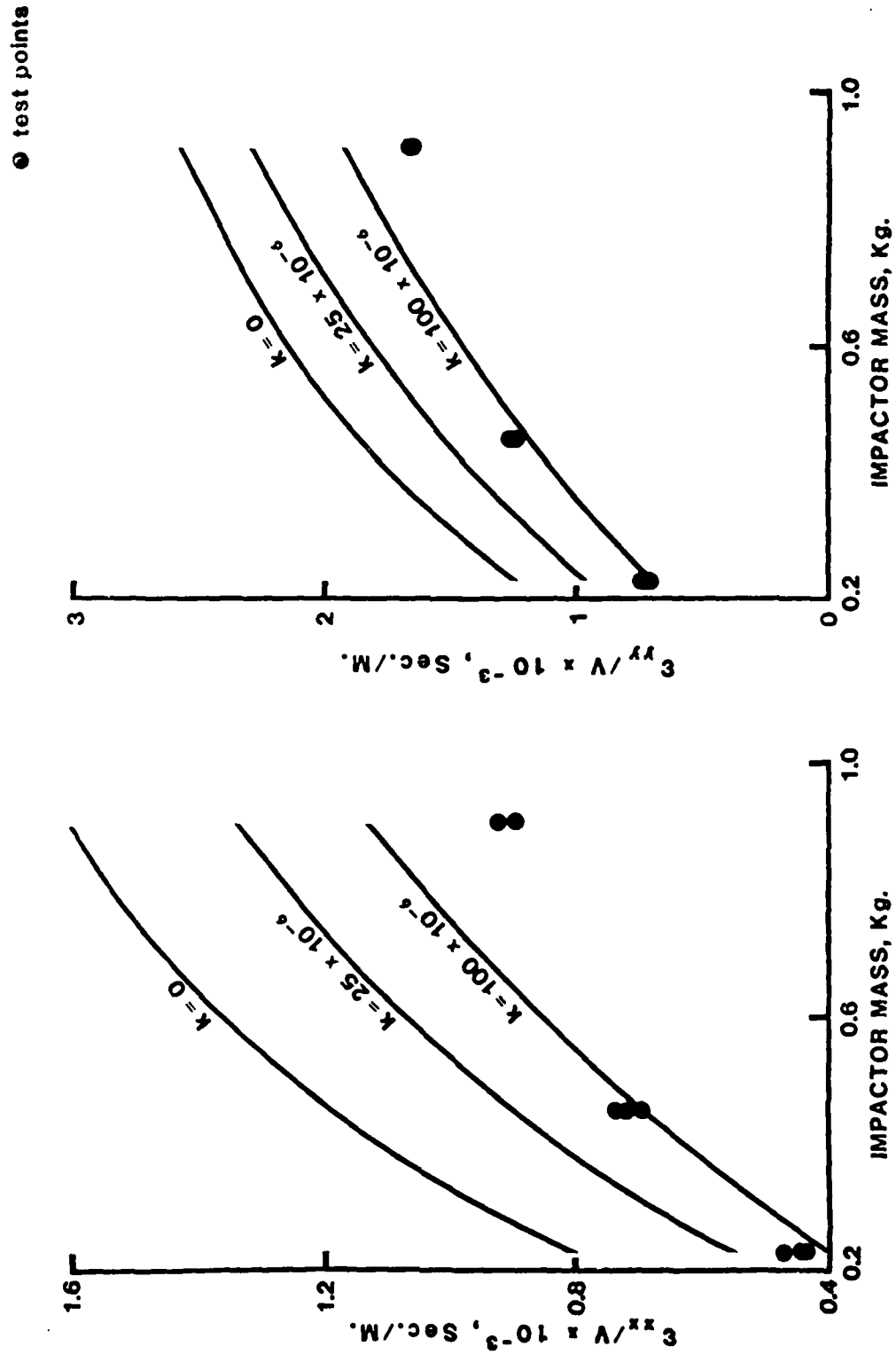

Figure 11 – Comparison Between Theoretical and Experimental Results for Plate F3

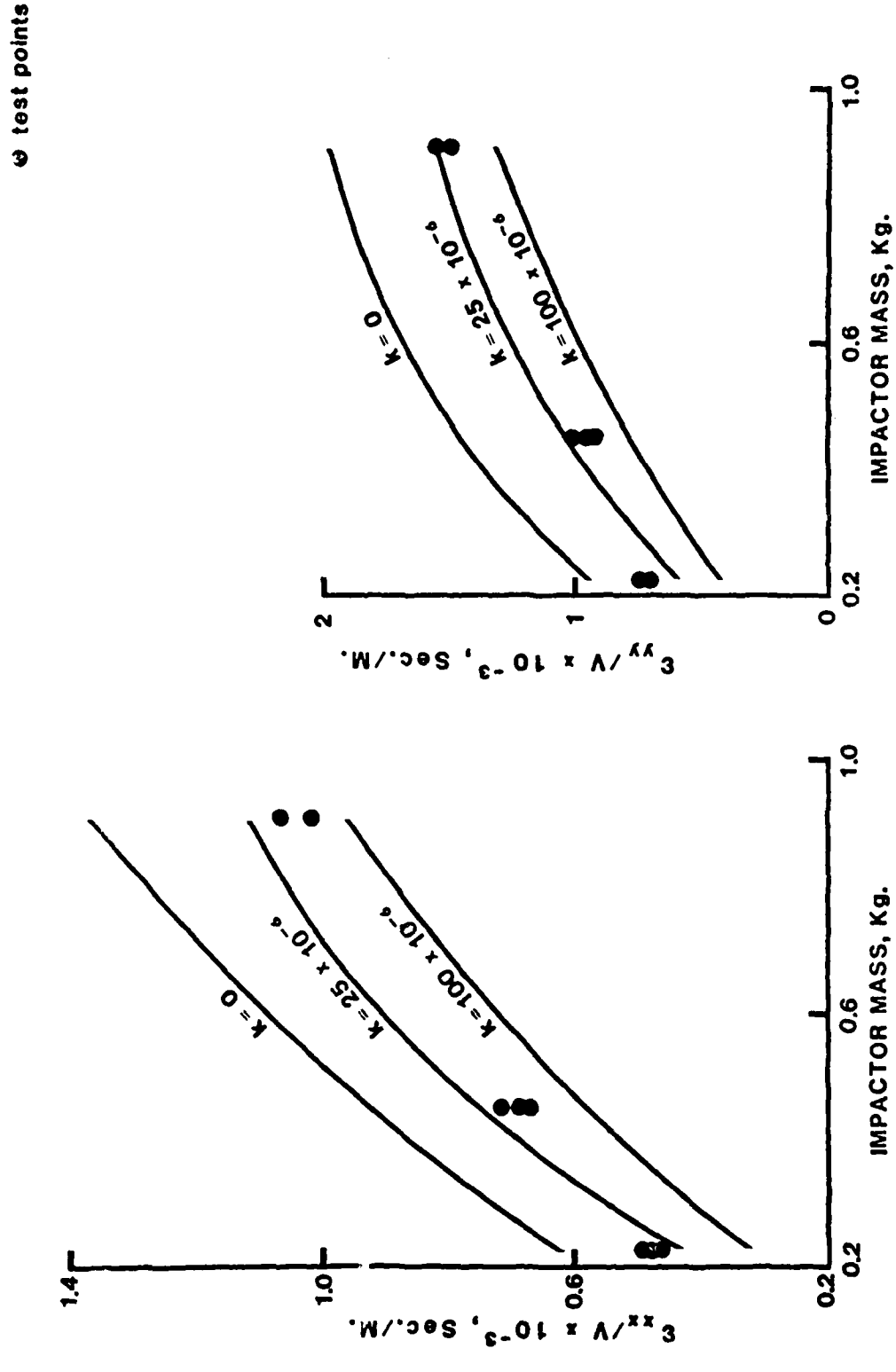

Figure 12 – Comparison Between Theoretical and Experimental Results for Pla . F4

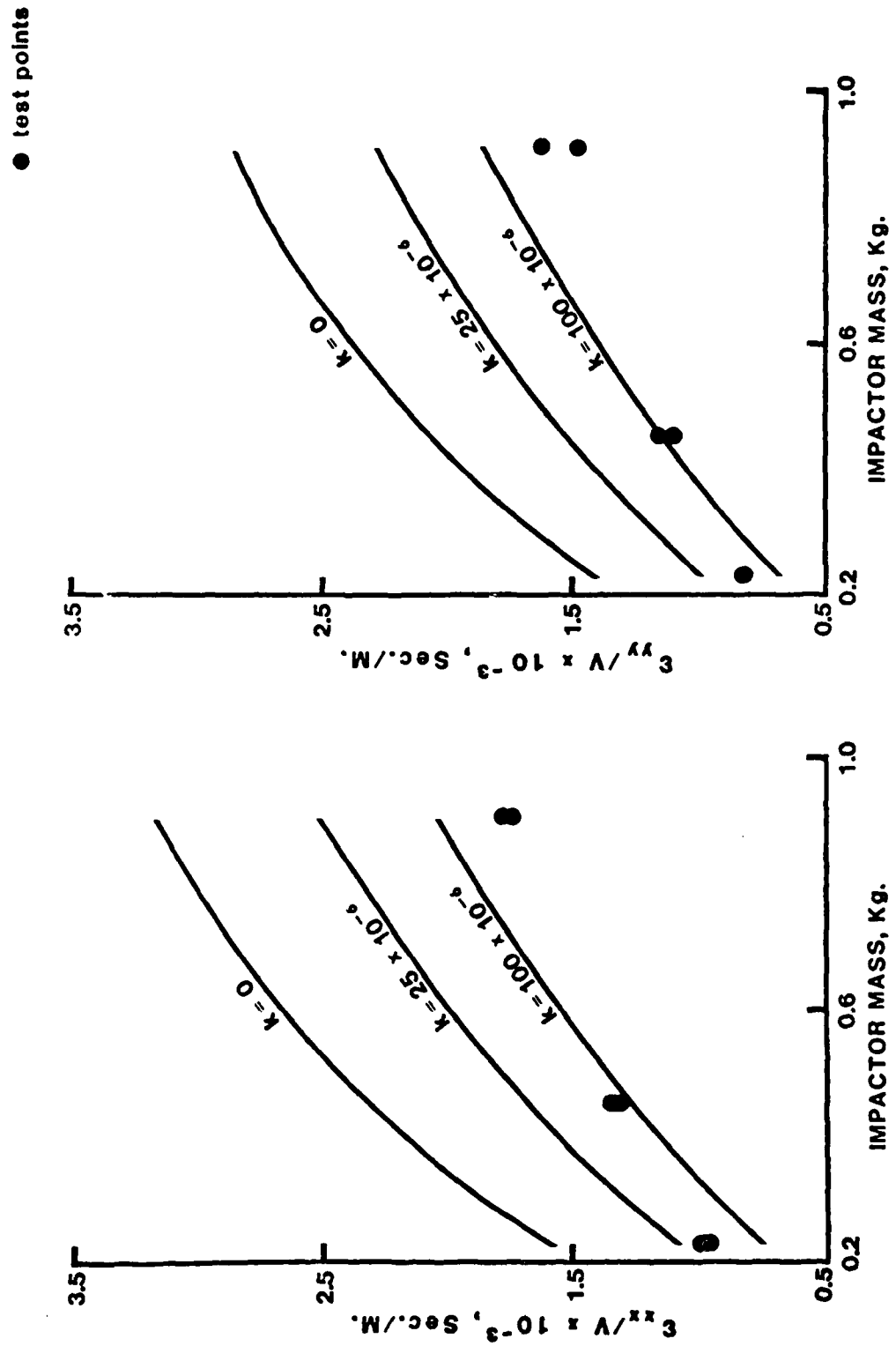

Figure 13 – Comparison Between Theoretical and Experimental Results for Plate H1

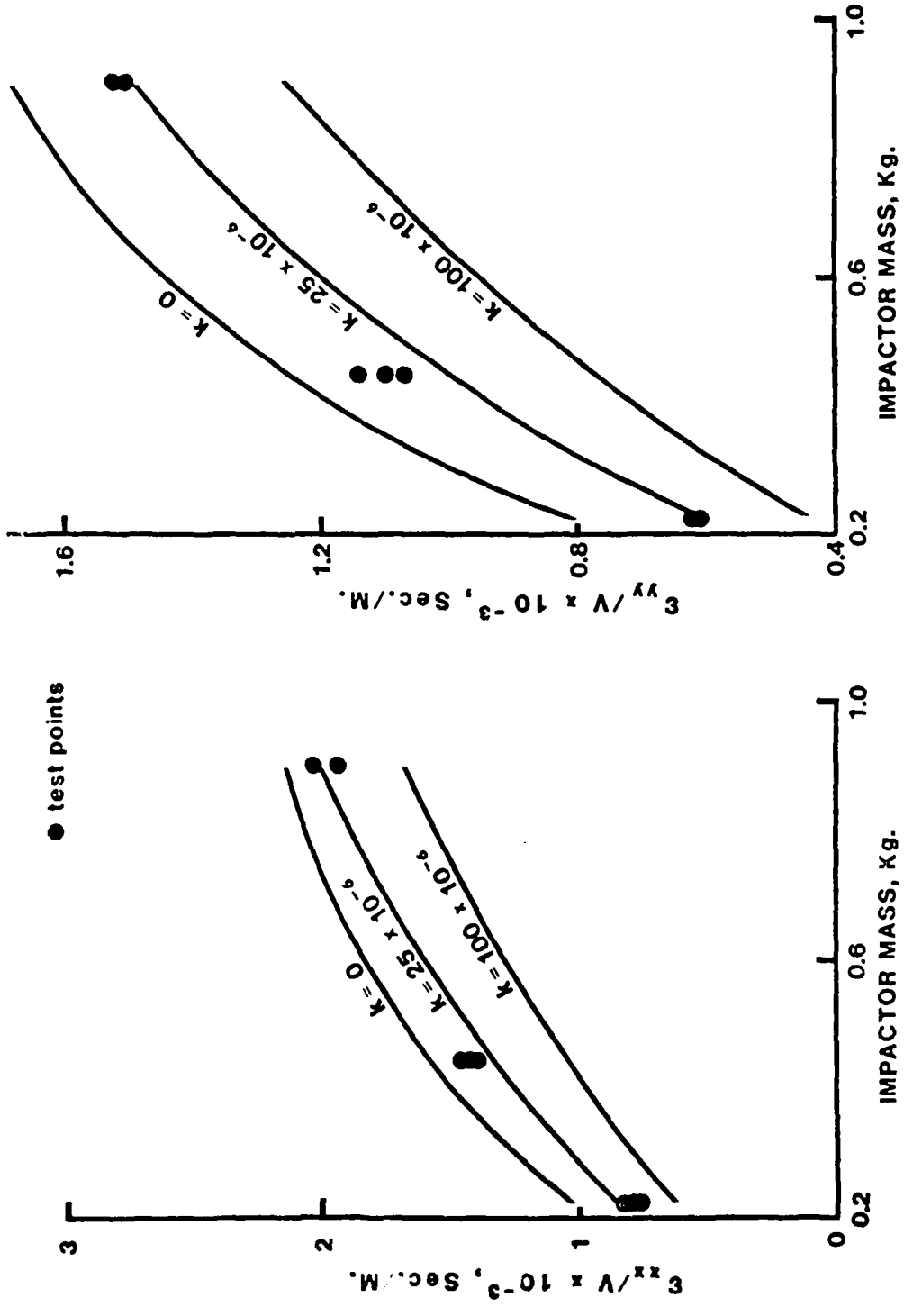

Figure 14 – Comparison Between Theoretical and Experimental Results for Plate H2

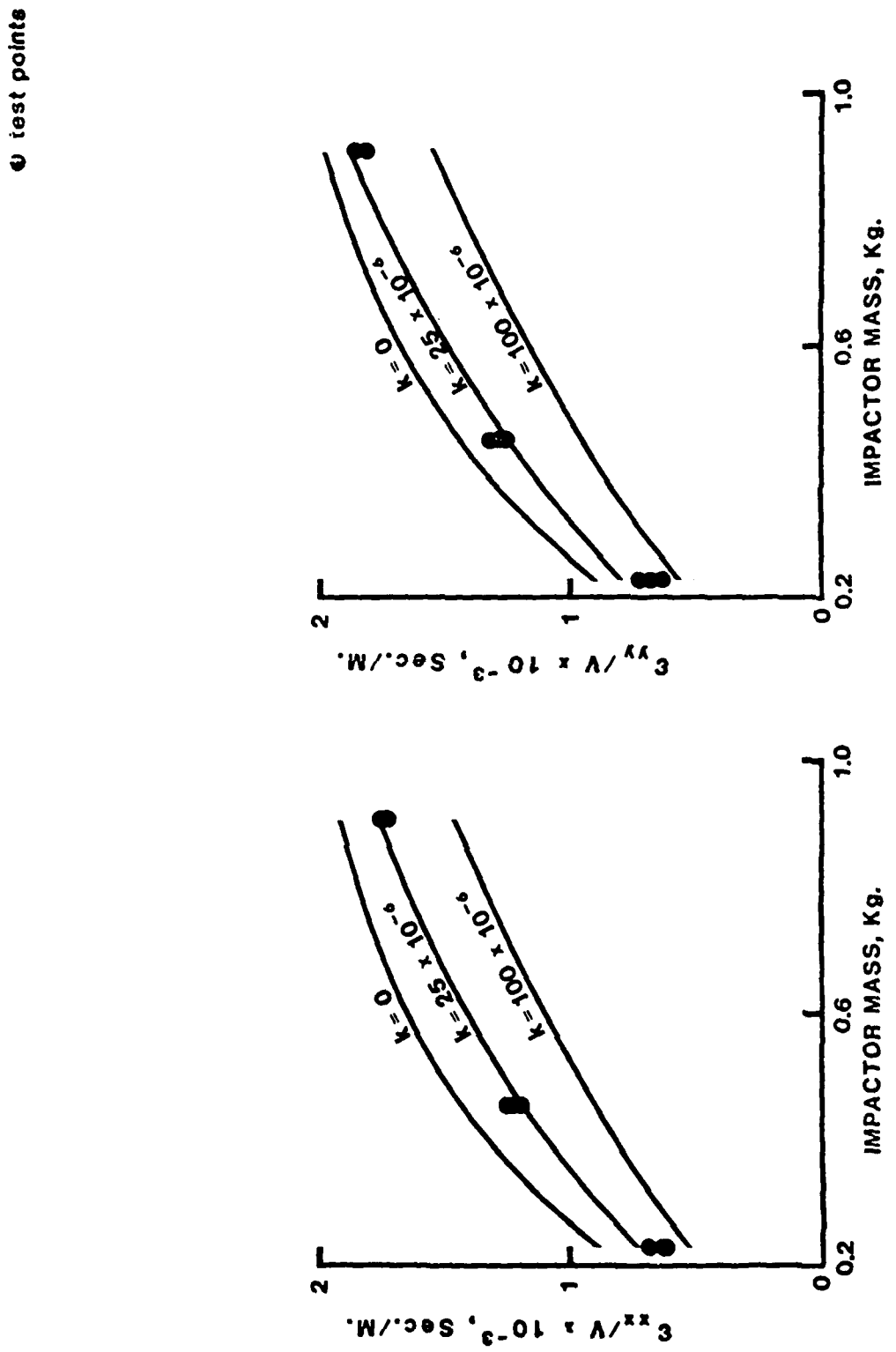

Figure 15 – Comparison Between Theoretical and Experimental Results for Plate H3

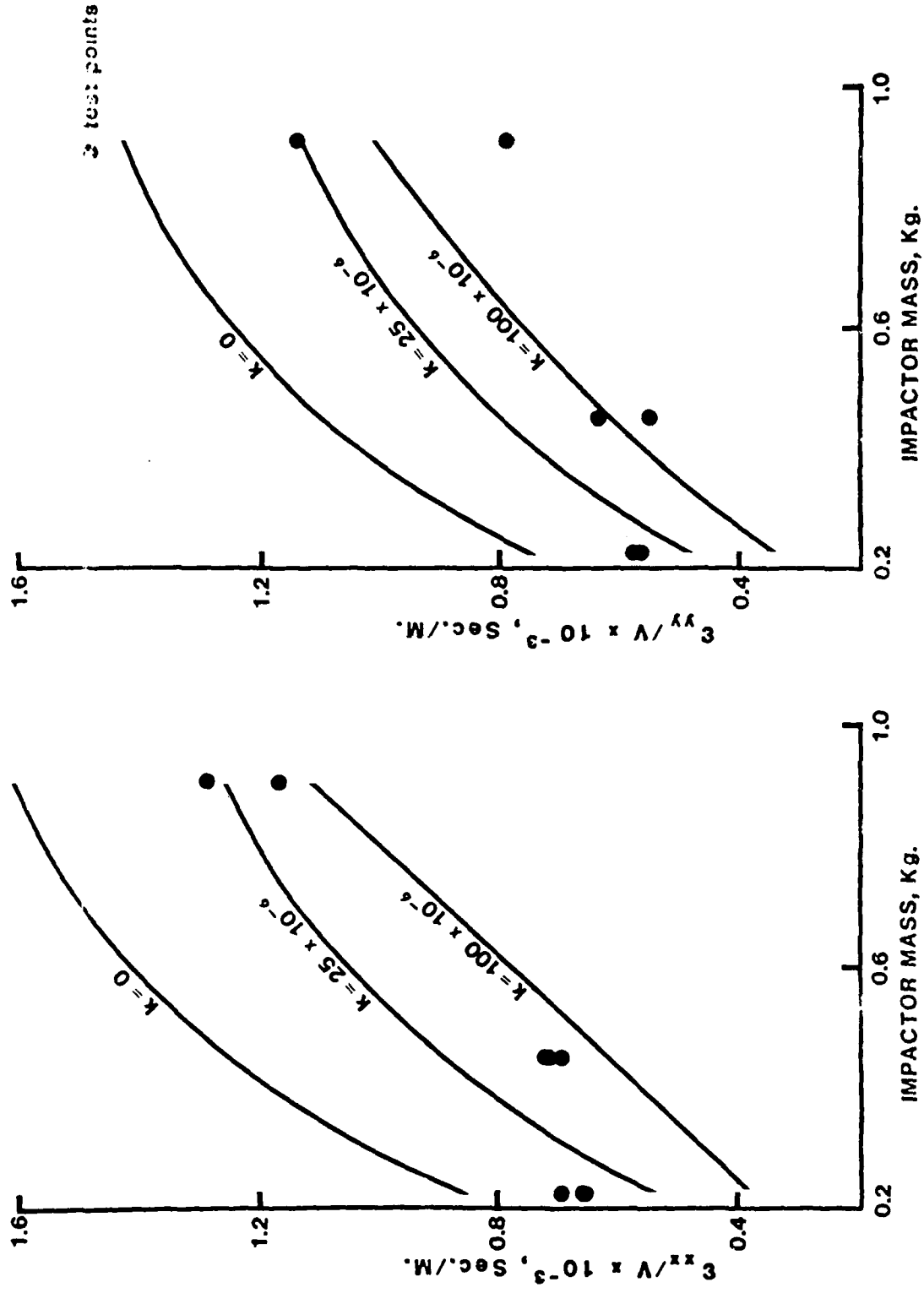

Figure 16 – Comparison Between Theoretical and Experimental Results for Plate H4

4.0 REFERENCES

1. McQuillen, E.J., Llorens, R.E. and Gause, L.W.

   "Low Velocity Transverse Normal Impact of Graphite Epoxy Composite Laminates", Report No. NADC-75119-30, Naval Air Development Center, Warminster, PA, June 1975.

2. Llorens, R.E. and McQuillen, E.J.

   "Off-Center, Low Velocity, Transverse Normal Impact of a Viscoelastic Beam", Report No. NADC-78237-60, Naval Air Development Center, Warminster, PA, Sep 1978.

3. Llorens, R.E. and McQuillen, E.J.

   "Off-Center, Low Velocity, Transverse Normal Impact of a Simple Supported Plate", Report No. NADC-79215-60, Naval Air Development Center, Warminster, PA, Sep 1979.

4. Chou, P.C., Flis, W.J. and Miller, H.

   "Certification of Composite Aircraft Structures Under Impact, Fatigue and Environmental Conditions – Part I – Low Speed Impact of Plates of Composite Materials", Report No. NADC-78259-60, Naval Air Development Center, Warminster, PA, Jan 1978.

APPENDIX A

STIFFNESS AND MASS MATRICES FOR A RECTANGULAR ELEMENT

A summarization of work which was performed in developing a finite element representation for both the stiffness and corresponding equivalent mass of an orthotropic plate.

We assume that the transverse deflection of the plate may be expressed as a polynomial of the following form,

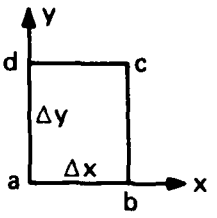

$$W = a_0 + a_1\tilde{\xi} + a_2\tilde{\eta} + a_3\tilde{\xi}^2 + a_4\tilde{\xi}\tilde{\eta} + a_5\tilde{\eta}^2 + a_6\tilde{\xi}^3 + a_7\tilde{\xi}^2\tilde{\eta} + a_8\tilde{\xi}\tilde{\eta}^2 + a_9\tilde{\eta}^3 + a_{10}\tilde{\xi}^3\tilde{\eta} + a_{11}\tilde{\xi}\tilde{\eta}^3 \quad \text{(A-1)}$$

where:

$a_0, a_1, \ldots, a_{11}$ = unknown constants

Δx = length of element

Δy = width of element

$$\tilde{\xi} = \frac{x}{\Delta x}$$

$$\tilde{\eta} = \frac{y}{\Delta y}$$

Utilizing the previous assumption, equation A-1, it may be shown that,

$$\alpha = a_1 + 2a_3\tilde{\xi} + a_4\tilde{\eta} + 3a_6\tilde{\xi}^2 + 2a_7\tilde{\xi}\tilde{\eta} + a_8\tilde{\eta}^2 + 3a_{10}\tilde{\xi}^2\tilde{\eta} + a_{11}\tilde{\eta}^3$$
$$\beta = a_2 + a_4\tilde{\xi} + 2a_5\tilde{\eta} + a_7\tilde{\xi}^2 + 2a_8\tilde{\xi}\tilde{\eta} + 3a_9\tilde{\eta}^2 + a_{10}\tilde{\xi}^3 + 3a_{11}\tilde{\xi}\tilde{\eta}^2 \quad \text{(A-2)}$$

where:

$$\alpha = W_{\tilde{\xi}}$$

$$\beta = W_{\tilde{\eta}}$$

Employing the expressions for W, α and β, equations (A-1) and (A-2), to determine the values of the unknown constants in terms of the deflections and rotations at the four corner points of the element, we find,

$$\begin{aligned} W = {} & (1-3\tilde{\xi}^2 - \tilde{\xi}\tilde{\eta} - 3\tilde{\eta}^2 + 2\tilde{\xi}^3 + 3\tilde{\xi}^2\tilde{\eta} + 3\tilde{\xi}\tilde{\eta}^2 + 2\tilde{\eta}^3 - 2\tilde{\xi}^3\tilde{\eta} - 2\tilde{\xi}\tilde{\eta}^3)W_a + \\ & (\tilde{\xi} - 2\tilde{\xi}^2 - \tilde{\xi}\tilde{\eta} + \tilde{\xi}^3 + 2\tilde{\xi}^2\tilde{\eta} - \tilde{\xi}^3\tilde{\eta})\alpha_a + \\ & (\tilde{\eta} - \tilde{\xi}\tilde{\eta} - 2\tilde{\eta}^2 + 2\tilde{\xi}\tilde{\eta}^2 + \tilde{\eta}^3 - \tilde{\xi}\tilde{\eta}^3)\beta_a + \\ & (3\tilde{\xi}^2 + \tilde{\xi}\tilde{\eta} - 2\tilde{\xi}^3 - 3\tilde{\xi}\tilde{\eta} - 3\tilde{\xi}\tilde{\eta}^2 + 2\tilde{\xi}^3\tilde{\eta} + 2\tilde{\xi}\tilde{\eta}^3)W_b + \\ & (-\tilde{\xi}^2 + \tilde{\xi}^3 + \tilde{\xi}^2\tilde{\eta} - \tilde{\xi}^3\tilde{\eta})\alpha_b + (\tilde{\xi}\tilde{\eta} - 2\tilde{\xi}\tilde{\eta}^2 + \tilde{\xi}\tilde{\eta}^3)\beta_b + \\ & (-\tilde{\xi}\tilde{\eta} + 3\tilde{\xi}^2\tilde{\eta} + 3\tilde{\xi}\tilde{\eta}^2 - 2\tilde{\xi}^3\tilde{\eta} - 2\tilde{\xi}\tilde{\eta}^3)W_c + \end{aligned} \quad \text{(A-3)}$$

$$(-\tilde{\xi}^2\tilde{\eta} + \tilde{\xi}^3\tilde{\eta})\alpha_c + (-\tilde{\xi}\tilde{\eta}^2 + \tilde{\xi}\tilde{\eta}^3)\beta_c +$$
$$(\tilde{\xi}\tilde{\eta} + 3\tilde{\eta}^2 - 3\tilde{\xi}^2\tilde{\eta} - 3\tilde{\xi}\tilde{\eta}^2 - 2\tilde{\eta}^3 + 2\tilde{\xi}^3\tilde{\eta} + 2\tilde{\xi}\tilde{\eta}^3)W_d + \quad \text{(A-3)}$$
$$(\tilde{\xi}\tilde{\eta} - 2\tilde{\xi}^2\tilde{\eta} + \tilde{\xi}^3\tilde{\eta})\alpha_d + (-\tilde{\eta}^2 + \tilde{\xi}\tilde{\eta}^2 + \tilde{\eta}^3 - \tilde{\xi}\tilde{\eta}^3)\beta_d$$

Note that subscripts on the variables W, α and β denote the corner point at which the corresponding quantity is to be evaluated. Thus, in view of equation (A-3) we may express the displacement W in the form,

$$W = G\Delta \quad \text{(A-4)}$$

where:

G = matrix relating transverse displacement W to the degrees of freedom of the nodes

Δ = vector of nodal degrees of freedom

The potential energy of a finite element assumes a form identical with equation (1), however, it is necessary to limit the integration to the domain of the element to obtain the correct result. Converting the integral to dimensionless variables and introducing the expression for W, equation (A-1), into the potential energy expression, equation (1), we find,

$$PE = \frac{1}{2}\Delta^T\left\{\frac{\Delta y}{\Delta x^3} D_{11}\int_0^1\int_0^1 G_{\tilde{\xi}\tilde{\xi}}^T G_{\tilde{\xi}\tilde{\xi}}\, d\tilde{\xi}\, d\tilde{\eta} + \right.$$
$$\frac{2}{\Delta x\Delta y} H\int_0^1\int_0^1 G_{\tilde{\xi}\tilde{\eta}}^T G_{\tilde{\xi}\tilde{\eta}}\, d\tilde{\xi}\, d\tilde{\eta} + \frac{\Delta x}{\Delta y^3} D_{22}\int_0^1\int_0^1 G_{\tilde{\eta}\tilde{\eta}}^T$$
$$\left. G_{\tilde{\eta}\tilde{\eta}}\, d\tilde{\xi}\, d\tilde{\eta}\right\}\Delta$$

Observe that subscripts appended to the matrix G are intended to denote differentiation with respect to the dimensionless variable indicated. Since $PE = \frac{1}{2}\Delta^T\hat{K}\Delta$, the previous equation implies that,

$$\hat{K} = \frac{\Delta y}{\Delta x^3} D_{11}\int_0^1\int_0^1 G_{\tilde{\xi}\tilde{\xi}}^T G_{\tilde{\xi}\tilde{\xi}}\, d\tilde{\xi}\, d\tilde{\eta} + \frac{2}{\Delta x\Delta y} H\int_0^1\int_0^1 G_{\tilde{\xi}\tilde{\eta}}^T G_{\tilde{\xi}\tilde{\eta}}$$
$$d\tilde{\xi}\, d\tilde{\eta} + \frac{\Delta x}{\Delta y^3} D_{22}\int_0^1\int_0^1 G_{\tilde{\eta}\tilde{\eta}}^T G_{\tilde{\eta}\tilde{\eta}}\, d\tilde{\xi}\, d\tilde{\eta} \quad \text{(A-5)}$$

where:

$\hat{K}$ = stiffness matrix

Further, we note that the maximum kinetic energy of a finite element also adopts a form identical with equation (5), however, it is necessary to limit the integration to the domain of the element. Therefore, if we introduce equation (A-4) into the maximum kinetic energy expression, equation (5), we conclude that,

$$KE_{max} = \frac{1}{2}\omega^2 \Delta^T \rho h \int_A G^T G \, dA \cdot \Delta$$

Recalling that $KE_{max} = \frac{1}{2}\omega^2 \Delta^T \hat{M} \Delta$, the previous result implies that

$$\hat{M} = \rho h \int_A G^T G \, dA = \rho h \, \Delta x \, \Delta y \int_0^1 \int_0^1 G^T G \, d\tilde{\xi} \, d\tilde{\eta} \qquad \text{(A-6)}$$

where:

$\hat{M}$ = equivalent mass matrix

Equations (A-5) and (A-6) formed the basis for the determination of the stiffness and equivalent mass matrices. As a part of this task, the G matrix was introduced into the two previously mentioned expressions. Since the elements of G include variables the integrations indicated in the definitions of the stiffness and mass matrices were performed by employing numerical integration techniques.

APPENDIX B

DETERMINATION OF APPROXIMATIONS FOR THE FIRST AND SECOND NATURAL FREQUENCIES

A summarization of calculations which were employed in constructing a computer program to obtain approximations for the first and second natural frequencies of a clamped plate.

FIRST MODE CALCULATIONS

For the problem under consideration, we shall assume the first mode may be represented in the form,

$$\overline{w}_1 = f(\zeta)\, g(\eta) \tag{B-1}$$

where:

$$f = (1 - \zeta^2)^2 (1 + \tilde{a}_0 \zeta^2 + \tilde{a}_1 \zeta^4)$$

$$g = (1 - \eta^2)^2 (1 + \tilde{b}_0 \eta^2 + \tilde{b}_1 \eta^4)$$

$\tilde{a}_0$, $\tilde{a}_1$, $\tilde{b}_0$ and $\tilde{b}_1$ = arbitrary constants

Utilizing equation (B-1), the previously indicated integrals in equation (6) reduce to the form,

$$\int_0^1 \int_0^1 \overline{w}_1^2 \, d\zeta \, d\eta = \int_0^1 f^2 \, d\zeta \int_0^1 g^2 \, d\eta$$

$$\int_0^1 \int_0^1 \overline{w}_{1\zeta\zeta}^2 \, d\zeta \, d\eta = \int_0^1 f_{\zeta\zeta}^2 \, d\zeta \int_0^1 g^2 \, d\eta$$

$$\int_0^1 \int_0^1 \overline{w}_{1\zeta\eta}^2 \, d\zeta \, d\eta = \int_0^1 f_\zeta^2 \, d\zeta \int_0^1 g_\eta^2 \, d\eta$$

$$\int_0^1 \int_0^1 \overline{w}_{1\eta\eta} \, d\zeta \, d\eta = \int_0^1 f^2 \, d\zeta \int_0^1 g_{\eta\eta}^2 \, d\eta$$

Note that subscripts appended to the deflection W_1 are employed to denote differentiation with respect to the dimensionless variable indicated.

In view of the symmetric nature of the f and g functions we need only record the following results,

$$\int_0^1 f^2 \, d\zeta = \frac{128}{315} \left\{ 1 + \frac{2}{11} \left(\tilde{a}_0 + \frac{3}{13} \tilde{a}_1 \right) + \frac{1}{143} \left(3\tilde{a}_0^2 + 2\tilde{a}_0 \tilde{a}_1 + \frac{7}{17} \tilde{a}_1^2 \right) \right\}$$

$$\int_0^1 f_\zeta^2 \, d\zeta = \frac{128}{105}\left\{1 - \frac{2}{33}\,\tilde{a}_1 + \frac{1}{429}\,(39\tilde{a}_0^2 + 28\tilde{a}_0\,\tilde{a}_1 + 9\tilde{a}_1{}^2)\right\}$$

$$\int_0^1 f_{\zeta\zeta}^2 \, d\zeta = \frac{64}{5}\left\{1 + \frac{2}{7}\,(\tilde{a}_0 + \frac{1}{3}\tilde{a}_1) + \frac{1}{7}(3\tilde{a}_0^2 + \frac{106}{33}\,\tilde{a}_0\,\tilde{a}_1 + \frac{643}{429}\,\tilde{a}_1{}^2)\right\}$$

SECOND MODE CALCULATIONS

For the second mode we shall assume the deflection is given by,

$$\overline{w_2} = (1 - \zeta^2)^2 (1 - \eta^2)^2 (1 - r_1\zeta^2 - r_2\eta^2)(1 + s_0\zeta^2 + s_1\zeta^4) \cdot \bullet(1 + t_0\eta^2 + t_1\eta^4) \qquad \text{(B-2)}$$

where:

r_1, r_2, s_0, s_1, t_0 and t_1 = arbitrary constant

We may express equation (B-2) in the following equivalent form,

$$\overline{w_2} = g(\zeta)\,h(\eta) - p(\zeta)\,q(\eta)$$

where:

$$g(\zeta) = (1 - \zeta^2)^2 (1 - r_1\zeta^2)(1 + s_0\zeta^2 + s_1\zeta^4)$$

$$h(\eta) = (1 - \eta^2)^2 (1 - r_2\eta^2)(1 + t_0\eta^2 + t_1\eta^4)$$

$$p(\zeta) = r_1\zeta^2 (1 - \zeta^2)^2 (1 + s_0\zeta^2 + s_1\zeta^4)$$

$$q(\eta) = r_2\eta^2 (1 - \eta^2)^2 (1 + t_0\eta^2 + t_1\eta^4)$$

Thus, introducing this last result into the integrals in equation (6), we obtain,

$$\int_A W_2^2 \, dA = \int g^2 \, d\zeta \int h^2 \, d\eta - 2\int g\,p\,d\zeta \int h\,q\,d\eta + \int p^2 \, d\zeta \int q^2 \, d\eta$$

$$\int_A W_{2\zeta\eta}^2 \, dA = \int g'^2 \, d\zeta \int h'^2 \, d\eta - 2\int g'\,p'\,d\zeta \int h'\,q'\,d\eta + \int p'^2 \, d\zeta \int q'^2 \, d\eta$$

$$\int_A W_{2\xi\xi}^2 \, dA = \int g''^2 \, d\xi \int h^2 \, d\eta - 2 \int g'' \, p'' \, d\xi \int h \, q \, d\eta + \int p''^2 \, d\xi \int q^2 \, d\eta$$

$$\int_A W_{2\eta\eta}^2 \, dA = \int g^2 \, d\xi \int h''^2 \, d\eta - 2 \int g \, p \, d\xi \int h'' \, q'' \, d\eta + \int p^2 \, d\xi \int q''^2 \, d\eta$$

Note that primes denote the derivative of the function with respect to the independent variable. Finally, determination of the values of the above integrals require the following information.

$$\int_0^1 g^2 \, d\xi$$

$$= \Big\{(2.903185E\text{-}4*r_1^2 - 1.108489E\text{-}3*r_1 + 1.170071E\text{-}3)\, s_1^2$$

$$+ [(1.108489E\text{-}3*r_1^2 - 4.680287E\text{-}3*r_1 + 5.683205E\text{-}3)\, s_0$$

$$+ 2.340143E\text{-}3*r_1^2 - 1.136641E\text{-}2*r_1 + 1.704961E\text{-}2]\, s_1$$

$$+ (1.170071E\text{-}3*r_1^2 - 5.683205E\text{-}3*r_1 + 8.524808E\text{-}3)\, s_0^2$$

$$+ (5.683205E\text{-}3*r_1^2 - 3.409923E\text{-}2*r_1 + 7.388167E\text{-}2)\, s_0$$

$$+ 8.524808E\text{-}3*r_1^2 - 7.388167E\text{-}2*r_1 + 4.063492E\text{-}1\Big\}$$

$$\int_0^1 p^2 \, d\xi$$

$$= 2.903185E\text{-}4*s_1^2 + (1.108489E\text{-}3*s_0 + 2.340143E\text{-}3)\, s_1$$

$$+ 1.170071E\text{-}3*s_0^2 + 5.683205E\text{-}3*s_0 + 8.524808E\text{-}3$$

$$\int_0^1 g \, p \, d\xi$$

$$= -\Big\{(2.903185E\text{-}4*r_1 - 5.542445E\text{-}4)\, s_1^2$$

$$+ [(1.108489E\text{-}3*r_1 - 2.340143E\text{-}3)\, s_0$$

$$+ 2.340143E\text{-}3*r_1 - 5.683205E\text{-}3]\, s_1$$

$$+ (1.170071E\text{-}3 * r_1 - 2.841602E\text{-}3)\, s_0^2$$

$$+ (5.683205E\text{-}3 * r_1 - 1.704961E\text{-}2)\, s_0$$

$$+ 8.524808E\text{-}3 * r_1 - 3.694083E\text{-}2 \Big\}$$

$$\int_0^1 (g')^2\, d\zeta$$

$$= \Big\{ (9.791653E\text{-}3 * r_1^2 - 2.808172E\text{-}2 * r_1 + 2.557442E\text{-}2)\, s_1^2$$

$$+ [(2.808172E\text{-}2 * r_1^2 - 7.956487E\text{-}2 * r_1 + 7.956487E\text{-}2)\, s_0$$

$$+ 2.841602E\text{-}2 * r_1^2 - 2.273282E\text{-}2 * r_1 - 7.388167E\text{-}2]\, s_1$$

$$+ (2.557442E\text{-}2 * r_1^2 - 7.956487E\text{-}2 * r_1 + 1.108225E\text{-}1) s_0^2$$

$$+ (7.956487E\text{-}2 * r_1^2 - 1.477633E\text{-}1 * r_1)\, s_0$$

$$+ 1.108225E\text{-}1 * r_1^2 + 1.219047 \Big\}$$

$$\int_0^1 (p')^2\, d\zeta$$

$$= 9.791653E\text{-}3 * s_1^2 + (2.808172E\text{-}2 * s_0 + 2.841602E\text{-}2)\, s_1$$

$$+ 2.557442E\text{-}2 * s_0^2 + 7.956487E\text{-}2 * s_0 + 1.108225E\text{-}1$$

$$\int_0^1 p'\, g'\, d\zeta$$

$$= - \Big\{ (9.791653E\text{-}3 * r_1 - 1.404086E\text{-}2)\, s_1^2$$

$$+ [(2.808172E\text{-}2 * r_1 - 3.978243E\text{-}2)\, s_0$$

$$+ 2.841602E\text{-}2 * r_1 - 1.136641E\text{-}2]\, s_1$$

$$+ (2.557442E\text{-}2 * r_1 - 3.978243E\text{-}2)\, s_0^2$$

$$+ (7.956487E\text{-}2 * r_1 - 7.388167E\text{-}2)\, s_0$$

$$+ 1.108225E\text{-}1 * r_1 \Big\}$$

$$\int_0^1 (g'')^2\, d\zeta$$

$$= \Big\{ (1.869189 * r_1^2 - 4.134532 * r_1 + 2.740725)\, s_1^2$$

$$+ [(4.134532 * r_1^2 - 8.848751 * r_1 + 5.873593)\, s_0$$

$$+ 3.367299 * r_1^2 - 6.427705 * r_1 + 1.219047]\, s_1$$

$$+ (2.740725 * r_1^2 - 5.873593 * r_1 + 5.485714)\, s_0^2$$

$$+ (5.873593 * r_1^2 - 1.219047E1 * r_1 + 3.657142)\, s_0$$

$$+ 5.485714 * r_1^2 - 3.657142 * r_1 + 1.280000E1 \Big\}$$

$$\int_0^1 (p'')^2\, d\zeta$$

$$= 1.869189 * s_1^2 + (4.134532 * s_0 + 3.367299)\, s_1$$

$$+ 2.740725 * s_0^2 + 5.873593 * s_0 + 5.485714$$

$$\int_0^1 g''\, p''\, d\zeta$$

$$= - \Big\{ (1.869189 * r_1 - 2.067266)\, s_1^2$$

$$+ [(4.134532 * r_1 - 4.424375)\, s_0$$

$$+ 3.367299 * r_1 - 3.213852]\, s_1$$

$$+ (2.740725*r_1 - 2.936796)\, s_0^2$$

$$+ (5.873593*r_1 - 6.095238)\, s_0$$

$$+ 5.485714*r_1 - 1.828571 \Big\}$$

ORTHOGONALITY RELATION

To reduce the complexity of the search procedure in the case of the second mode we utilized the orthogonality relation. Specifically, this converted the problem from that of determining an extreme value to that of determining an absolute minimum over the space under consideration. The computer program which utilized this relation proved to be computationally rapid and convenient.

Let us consider the following integral,

$$\int_A \overline{w}_1\, \overline{w}_2\, dA = \int g_0(\zeta)\, g(\zeta)\, d\zeta \int h_0(\eta)\, h(\eta)\, d\eta$$

$$- \int g_0(\zeta)\, p(\zeta)\, d\zeta \int h_0(\eta)\, g(\eta)\, d\eta$$

where:

$$g_0(\zeta) = (1 - \zeta^2)^2\, (1 + \tilde{a}_0\, \zeta^2 + \tilde{a}_1\, \zeta^4)$$

$$h_0(\eta) = (1 - \eta^2)^2\, (1 + \tilde{b}_0\, \eta^2 + \tilde{b}_1\, \eta^4)$$

It may be shown that,

$$\int g_0 g\, d\zeta = - \{d_0 * r_1 - d_1\}$$

$$\int g_0 p\, d\zeta = d_0$$

where:

$$d_0 = (2.841602E\text{-}3 + 1.170071E\text{-}3*\tilde{a}_0 + 5.542445E\text{-}4*\tilde{a}_1)*s_1$$
$$+ (8.524808E\text{-}3 + 2.841602E\text{-}3*\tilde{a}_0 + 1.170071E\text{-}3*\tilde{a}_1)*s_0$$
$$+ 3.694083E\text{-}2 + 8.524808E\text{-}3*\tilde{a}_0 + 2.841602E\text{-}3*\tilde{a}_1$$

$$d_1 = (8.524808E\text{-}3 + 2.841602E\text{-}3*\tilde{a}_0 + 1.170071E\text{-}3*\tilde{a}_1)*s_1$$
$$+ (3.694083E\text{-}2 + 8.524808E\text{-}3*\tilde{a}_0 + 2.841602E\text{-}3*\tilde{a}_1)*s_0$$
$$+ 4.063492E\text{-}1 + 3.694083E\text{-}2*\tilde{a}_0 + 8.524808E\text{-}3*\tilde{a}_1$$

For the present circumstance the orthogonality relation may be written in the form,

$$\int \overline{w}_1 \overline{w}_2 \, dA + \frac{\tilde{M}/4}{\rho h} = 0$$

Employing the previous two sets of equations recorded in this section, we obtain,

$$d_0 e_1 r_1 + d_1 e_0 r_2 = d_1 e_1 + \frac{\tilde{M}/4}{\rho hab}$$

where:

e_0, e_1 represent factors identical with d_0, d_1 except that the constants $\tilde{a}_0$, $\tilde{a}_1$ are replaced by $\tilde{b}_0$, $\tilde{b}_1$ and s_0, s_1 by t_0, t_1.

Finally, we transform this last expression to the following more computationally convenient form,

$$r_1 = \Theta \, (d_1 e_1 + \frac{\tilde{M}/4}{\rho hab}) / (d_0 e_1)$$

$$r_2 = (1 - \Theta) \cdot (d_1 e_1 + \frac{\tilde{M}/4}{\rho hab}) / (d_1 e_0)$$

where:

Θ = arbitrary variable

APPENDIX C

NUMERICAL APPROXIMATION TO INTEGRATION

A record of the effort which was expended in producing a technique for the approximate integration of an arbitrary function. Included in the description is a summary of those modifications of the basic procedure which are indicated as a consequence of the symmetries inherent in the problem.

We shall develop an approximation for an arbitrary function by utilizing the twelve points indicated in the figure. For convenience, we express the nodal position in the x direction in units of h and in the y direction in units of k. Therefore, let us attempt to represent the arbitrary function f over the x-y plane by the following polynomial,

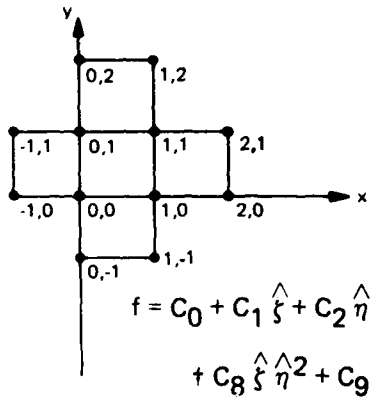

$$f = C_0 + C_1\hat{\xi} + C_2\hat{\eta} + C_3\hat{\xi}^2 + C_4\hat{\xi}\hat{\eta} + C_5\hat{\eta}^2 + C_6\hat{\xi}^3 + C_7\hat{\xi}^2\hat{\eta}$$
$$+ C_8\hat{\xi}\hat{\eta}^2 + C_9\hat{\eta}^3 + C_{10}\hat{\xi}^3\hat{\eta} + C_{11}\hat{\xi}\hat{\eta}^3$$

where $\hat{\xi} = \frac{x}{h}$

$\hat{\eta} = \frac{y}{k}$

It may be shown that the integration of the above function over the center square in terms of the values of the function at the nodal points is given by,

$$\int_0^h \int_0^k f\,dx\,dy = \frac{1}{48}\,hk\,\left\{14\,(f_{1,1} + f_{1,0} + f_{0,1} + f_{0,0}) - (f_{2,1} + f_{1,2} + f_{2,0} + f_{0,2} + f_{1,-1} + f_{-1,1} + f_{-1,0} + f_{0,-1})\right\}$$

where $f_{i,j}$ = value of the arbitrary function f at node i, j.

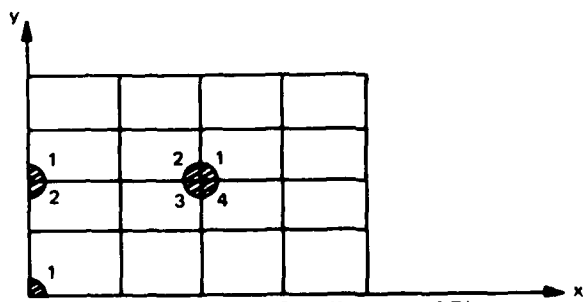

Finite Element Subdivision of Plate

Next, let us consider the computational difficulties associated with the subdivision of the quarter plate in accord with the pattern established in the attached figure. Since our basic integration pattern utilizes nodal points of the finite element it may be shown that corner points of the finite element subdivision satisfy the following constraints,

1. Only one finite element corner point occurs at the four corner points of the quarter plate.

2. Two finite element corner points are found to occur at each point lying along the exterior edges of the quarter plate.

3. Four finite element corner points coincide with each interior point of the quarter plate.

If we extend the above declarations to account for the effects of the integration pattern in the region under consideration, recalling the symmetry conditions which are applicable to our physical problem, we conclude that,

1. The four corner points of the quarter plate occur two times.

2. Finite element corner points which lie along an edge of the quarter plate occur four times.

3. All finite element corner points which lie in the interior of the quarter plate occur eight times.

Considering this latter information it may be shown that the application of the previously recorded integration formula to the integration of any function over the quarter plate is given by,

$$\int_A f dA = \frac{1}{4} hK \left\{ \Sigma f_{corner} + 2\Sigma f_{edge} + 4\Sigma f_{interior} \right\}$$

where f corner = f evaluated at corner point

f edge = f evaluated at edge point

f interior = f evaluated at interior point

No. of Copies

Rockwell International, Columbus, OH 43216
(Attn: Mr. F. Kaufman, Mr. M. Schweiger) 2
Rockwell International, Los Angeles, CA 90053 (Attn: Dr. Lackman) 1
Rockwell International, Tulsa OK 74151
(Attn: Mr. E. Sanders, Mr. J. H. Powell) 2
Owens Corning Fiberglass, Granville, OH 43023
(Attn: Mr. D. Mettes) 1
Rohr Corporation, Riverside, CA 92503
(Attn: Dr. F. Riel and Mr. R. Elkin) 2
Ryan Aeronautical Company, San Diego, CA 92112
(Attn: Mr. R. Long) 1
Sikorsky Aircraft, Stratford, CT 06497
(Attn: Mr. J. Ray) 1
University of Oklahoma, Norman, OK 93069
(Attn: Dr. C. W. Bert, School of AMNE) 1
Union Carbide Corporation, Cleveland, OH 44101
(Attn: Dr. H. F. Volk) 1
University of Wyoming, Laramie, WY 82071 (Attn: Dr. D. F. Adams) 1
Virginia Polytechnic Institute, Blacksburg, VA 24061
(Dr. K Reifsnider) 1
Villanova University, Phila., PA 19085 (Dr. P. V. McLaughlin) 1
Vought Corporation, Dallas, TX 75222
(Attn: Mr. O. E. Dhonau/2-53442, Dr. J. Renton) 2
Compositek Engineering Corporation, 6925-1 Aragon Circle,
Buena Park, CA 90620 (Attn: J. V. Noyes) 1
University of Dayton Research Institute, 300 College Park Ave.,
Dayton, OH 45469 (Attn: Dr. J. Gallagher) 1

	No. of Copies
General Dynamics, Fort Worth, TX 76101	
(Attn: Mr. J. A. Fant, Mr. E. Petruska)	2
(Attn: Dr. D. Wilkins (Composite Structures Eng. Dept.))	1
General Electric Company, Phila., PA 19101	
(Attn: Dr. C. Zweben, Mr. A. Garber)	2
Great Lakes Carbon Corporation, NY, NY 10017	
(Attn: Mr. W. R. Benn, Mgr., Market Development)	1
School of Engineering and Applied Science, Materials Research Laboratory, Washington University, Campus Box 1087, St. Louis, MO 63130 (Attn: T. Hahn)	1
University of Delaware, Mechanics & Aerospace Eng. Dept., Evans Hall, Newark, DE 19711 (Attn: Dr. R. B. Pipes)	1
Prototype Development Associates, Inc., 1560 Brookhollow Drive, Santa Ana, CA 92705 (Attn: E. L. Stanton)	1
Grumman Aerospace Corporation, Bethpage, L.I., NY 11714	
(Attn: Mr. R. Hadcock, Mr. S. Dastin)	2
Hercules Powder Company, Inc., Cumberland, MD 21501	
(Attn: Mr. D. Hug)	1
H. I. Thompson Fiber Glass Company, Gardena, CA 90249	
(Attn: Mr. N. Myers)	1
ITT Research Institute, Chicago, IL 60616	
(Attn: Mr. K. Hofar)	1
J. P. Stevens & Co., Inc., NY, NY 10036	
(Attn: Mr. H. I. Shulock)	1
Kaman Aircraft Corporation, Bloomfield, CT 06002	
(Attn: Tech. Library)	1
Lehigh University, Bethlehem, PA 18015	
(Attn: Dr. G. C. Sih)	1
Lockheed-California Co., Burbank, CA 91520	
(Attn: Mr. E. K. Walker, Mr. Vaughn, Mr. A. James)	3
Lockheed-California Co., Rye Canyon Research Lab, Burbank, CA 91520 (Attn: Mr. Don E. Pettit)	1
Lockheed-Georgia Company, Marietta, GA 30063	
(Attn: Technical Information Dept., Dept. 72-34, Zone 26)	1
Martin Company, Baltimore, MD 21203	
(Attn: Mr. J. E. Pawken)	1
Materials Sciences Corporation, Blue Bell, PA 19422	1
McDonnell Douglas Corporation, St. Louis, MO 63166	
(Attn: Mr. J. Schier, C. Stenberg, R. Garrett)	3
McDonnell Douglas Corporation, Long Beach, CA 90801	
(Attn: G. Lehman, D. Smillie)	2
Minnesota Mining and Manufacturing Company, St. Paul, MN 55104	
(Attn: Mr. W. Davis)	1
Northrop Aircraft Corporation, One Northrop Ave., Hawthorne, CA 90250	
(Attn: Mr. L. Jeans, Mr. D. Stansbarger, Mr. R. C. Isemann, Mr. R. M. Verette, B. Butler)	5

No. of Copies

CONRL, Washington, D.C. 20375 Naval Research Laboratory
(Attn: Dr. I. Wolock) 1
CONAVAIRDEVCEN, Warminster, PA 18974
(Attn: Major J.C. Lillie - 097); 3 for Code 8131) 4
COONR, Washington, D.C. 20362 Office of Naval Research
(Attn: Dr. N. Perrone) 1
COPLASTEC, Picatinny Arsenal, Dover, NJ 07801
(Attn: Librarian, Bldg. 176, SARPA-FR-M-D and Mr. H. Pebly) 2
COApplied Technology Laboratory, USARTL (AVRADCOM) Ft. Eustis, VA
23604 (Attn: Mr. A.J. Gustafson, DAVDL-ATL-ATS, Mr. T. Mazza) 2
COAMMRC/DRXMR-TM, Watertown, MA 02172 Army Materials and Mechanics
Research Center (Attn: Dr. E. Lenoe, Mr. D. Oplinger) 2
COUSARESOFC, Durham, NC 27701 U.S. Army Research Office 1
COUSARTL (AVRADCOM) Ames Research Center, Moffett Field, CA 94035
U.S. Army R&T Laboratories (Attn: Mr. F. Immen, DAVDL-AS-M.S.
207-5, Dr. R. Foye) 2

Avco Aero Structures Division, Nashville, TN 37202 1
Batelle Columbus Laboratories, Metals and Ceramics Information
Center, 505 King Avenue, OH 43201 1
Bell Aerospace Company, Buffalo, NY 14240
(Attn: Zone I-85, Mr. F. M. Anthony) 1
Bell Helicopter Company, Fort Worth, TX 76100
(Attn: Mr. Charles Harvey) 1
Bendix Products Aerospace Division, South Bend, IN 46619
(Attn: Mr. R. V. Cervelli) 1
Boeing Aerospace Company, P.O. Box 3999, Seattle, WA 98124
(Attn: Code 206, Mr. R. E. Horton) 1
Boeing Company, P.O. Box 3707, Seattle, WA 98124-MS 6W-13
(Attn: Dr. R. June) 1
Boeing Company, Vertol Division, Phila., PA 19142
(Attn: Mr. R. L. Pickney, Mr. D. Hoffstedt, Mr. L. Marchinski) 3
Boeing Company, Wichita, KS 67210 (Attn: R. D. Hoaglanb - MS-K32-95) 1
Cabot Corporation, Billerica Research Center, Billerica, MA 01821 1
Drexel University, Phila., PA 19104
(Attn: Dr. P. C. Chou) 1
(Attn: Dr. A. S. D. Wang) 1
Effects Technology, Inc., 5383 Hollister Avenue, P. O. Box 30400,
Santa Barbara, CA 93105 (Attn: Robert Globus) 1
E. I. DuPont Company, Wilmington, DE 19898
(Attn: Dr. J. Pigoiacampi) 1
Fairchild Industries, Hagerstown, MD 21740
(Attn: Mr. D. Ruck) 1
Georgia Institute of Technology, Atlanta, GA
(Attn: Prof. W. H. Horton) 1
General Dynamics/Convair, San Diego, CA 92138
(Attn: Mr. D. R. Dunbar, W. G. Scheck) 2

DISTRIBUTION LIST

AIRTASK NO. WR0230301
Work Unit DG602

	No. of Copies
CONAVAIRSYSCOM, (AIR-950D), 2 for retention, 2 for AIR-530, 1 for AIR-320B, AIR-52032D, AIR-5302, AIR-53021, AIR-530215	9
COAFWAL, WPAFB, OH 45433	
(Attn: FIBEC, Dr. Geo. Sendeckyj	1
(Attn: FIB/Mr. L. Kelly, Mr. W. Goesch)	2
(Attn: FIBCA/Mr. C. D. Wallace)	1
(Attn: FIBAC/Mr. H. A. Wood)	1
(Attn: FIBE/Mr. D. Smith)	1
(Attn: MLBM/Dr. J. Whitney)	1
(Attn: MLB/Mr. Frank Cherry)	1
(Attn: MBC/Reinhart)	1
(Attn: MXA/Fecheck)	1
Dept. of the Air Force, Bldg. 410, Bolling Air Force Base, Wash., DC 20332 (Attn: Dr. M. Salkind)	1
DTIC	12
FAA, Washington, D.C. 20553 (Attn: R. Allen-AWS/120	1
FAA Technical Center, Atlantic City, N.J. 08405	
(Attn: Mr. D. W. Nesterok/Code ACT 330)	1
CONASA, Washington, D.C. 20546	
(Attn: Mr. Charles Bersh)	1
CONASA, George C. Marshall Space Flight Center, Huntsville, AL 35812	
(Attn: S&E-ASTN-ES/Mr. E. E. Engler)	1
(Attn: S&E-ASTN-M/Mr. R. Schwinghamer)	1
(Attn: S&E-ASTM-MNM/Dr. J. M. Stuckey)	1
CONASA, Langley Research Center, Hampton, VA 23365 (Attn: Dr. J. R. Davidson, M.S. 188E; Dr. J. Starnes, M.S. 190; Dr. J. Williams, M.S. 190, Dr. M. Mikulus, Mr. H. Bohan)	5
CONASA, Lewis Research Center, Cleveland, OH 44153 (Attn: Dr. C. Chamis, M.S. 49-6 and M. Hershberg)	2
CONAVPGSCHL, Monterey, CA 95940 (Attn: Prof. R. Ball, Prof. M. H. Bank, Prof. G. Lindsey)	3
CONAVSEASYSCOM, Crystal Mall 4, Rm. 109, Washington, D.C. 20360 (Attn: Dr. H. Vanderveldt)	1
CONAVSEC, Arlington, VA 20360 Naval Ship Engineering Center (Attn: NSEC-6101E)	1
CODTNAVSHIPRANDCEN, Bethesda, MD 20034 David Taylor Naval Ship Research and Development Denter (Attn: Code 173.2, Mr. W.P. Couch)	1
CODTNAVSHIPRANDCEN, Annapolis, MD 21402 David Taylor Naval Ship Research and Development Center (Attn: Code 2870, Mr. H. Edelstein)	1
CONOL, White Oak, MD 20910 Naval Ordance Laboratory (Attn: Mr. F.R. Barnet)	1